

J. W. JEWEL
PERSONAL COPY

NATIONAL ADVISORY COMMITTEE FOR AERONAUTICS

WARTIME REPORT

ORIGINALLY ISSUED

February 1946 as
Advance Confidential Report L5J29a

EFFECTS OF SPECIFIC TYPES OF SURFACE ROUGHNESS
ON BOUNDARY-LAYER TRANSITION

By Laurence K. Loftin, Jr.

Langley Memorial Aeronautical Laboratory
Langley Field, Va.

The NACA logo features the letters "NACA" in a bold, sans-serif font, centered within a stylized, wing-like shape that tapers at the ends. The logo is printed in black ink on a white background.

NACA

WASHINGTON

NACA WARTIME REPORTS are reprints of papers originally issued to provide rapid distribution of advance research results to an authorized group requiring them for the war effort. They were previously held under a security status but are now unclassified. Some of these reports were not technically edited. All have been reproduced without change in order to expedite general distribution.

NACA ACR No. L5J29a

NATIONAL ADVISORY COMMITTEE FOR AERONAUTICS

ADVANCE CONFIDENTIAL REPORT

EFFECTS OF SPECIFIC TYPES OF SURFACE ROUGHNESS
ON BOUNDARY-LAYER TRANSITION

By Laurence K. Loftin, Jr.

SUMMARY

Tests were conducted with two typical low-drag airfoils of 90-inch chord to determine the effects of surface projections, grooves, and sanding scratches on boundary-layer transition. The Reynolds number at which a spanwise row of cylindrical projections would cause premature transition was determined for a range of Reynolds number from approximately 3×10^6 to 10×10^6 . Data were obtained for projections of various sizes and chordwise locations on both low-drag airfoils. The results were analyzed on the assumption that the critical airfoil Reynolds number for a given projection was a function only of the local-flow conditions around the projection. This assumption neglected possible effects of tunnel turbulence, pressure gradient, boundary-layer Reynolds number, and the original extent of the laminar flow. The data correlated on the basis of this assumption within a range of critical airfoil Reynolds number of $\pm 0.5 \times 10^6$ and within a range of projection height of ± 0.002 inch. The tests of surface grooves and sanding scratches indicated that, for the range of Reynolds number investigated, the laminar boundary layer was much less sensitive to surface grooves and sanding scratches than to projections above the surface.

INTRODUCTION

The development of the NACA low-drag airfoils has aroused a great deal of interest in the problem of determining the amount of surface roughness necessary to cause premature boundary-layer transition from laminar to turbulent flow. A considerable amount of data has been published (references 1 and 2) pertaining to the effects

on airfoil characteristics of the application of carbondum grains to airfoil surfaces. Little data have been published, however, concerning the Reynolds number at which surface projections of a given size and chordwise location would cause premature transition. Fage has conducted tests to determine the allowable size of three forms of surface ridge - flat, arch, and wire - located at various positions on low-drag airfoils (references 3 and 4) and later extended the work to include the effect of smooth bulges and hollows (reference 5). Tani, Hama, and Mituisi (reference 6) have investigated the effect of spanwise wires on premature transition.

The purpose of the present investigation was to determine the Reynolds number at which surface projections of a given type but of various sizes and chordwise locations would cause premature transition and, if possible, to establish a general relation between the projection size and critical Reynolds number. An attempt was also made to determine the effects of sanding scratches and imperfect sheet-metal butt joints.

The tests of this investigation were conducted in the Langley two-dimensional low-turbulence tunnel. Two typical low-drag airfoils were tested and data were obtained for various combinations of projection size and chordwise location through a range of Reynolds number from approximately 3×10^6 to 10×10^6 . Data were also obtained with the airfoil surfaces finished with various grades of sandpaper and carborundum paper. The imperfect sheet-metal butt joints were simulated by grooves cut into the surface. Tests were made with spanwise grooves of various sizes and chordwise locations.

Although the projections tested simulated no definite type of roughness, the results of this investigation should prove useful as an indication of the order of magnitude of the individual specks that may be tolerated on a low-drag airfoil of given chord and pressure distribution. The Reynolds numbers of these tests were low compared with usual flight values; however, application of the analysis to the prediction of allowable projection sizes at higher Reynolds numbers appears reasonable, particularly for projections on the forward part of the airfoil.

SYMBOLS AND COEFFICIENTS

- c_d airfoil section drag coefficient
- y distance normal to surface of low-drag airfoil
- δ boundary-layer thickness, defined as that distance normal to the surface at which $\left(\frac{u}{U}\right)^2 = \frac{1}{2}$
- k height of projection
- d diameter of projection
- c chord of low-drag airfoil
- x distance from airfoil leading edge measured along chord line
- s distance from airfoil leading edge measured along surface
- U_0 free-stream velocity
- U local velocity just outside boundary layer
- u local velocity inside boundary layer
- u_k local velocity inside boundary layer at top of a projection
- q_0 free-stream dynamic pressure
- p local static pressure
- H local total pressure just outside boundary layer
- H_0 free-stream total pressure
- h local total pressure inside boundary layer
- S pressure coefficient $\left(\frac{H_0 - p}{q_0}\right)$
- ν coefficient of kinematic viscosity

- R airfoil Reynolds number; based on chord of low-drag airfoil and free-stream velocity $\left(\frac{U_{oc}}{v}\right)$
- R' Reynolds number per unit length; based on velocity just outside boundary layer $\left(\frac{U}{v}\right)$
- R_δ boundary-layer Reynolds number; based on boundary-layer thickness and local velocity just outside boundary layer (R'δ)
- R_k projection Reynolds number; based on height of projection and velocity in boundary layer at top of projection $\left(\frac{ku_k}{v}\right)$
- R_x Reynolds number based on distance x and local velocity just outside boundary layer at position x (R'x)
- T boundary-layer transition parameter $\left(\frac{\sqrt[3]{h-p}}{\sqrt{H-p}}\right)$
- A constant for any chordwise location of projection $\left(\frac{U_{oc}}{U}\right) \left(\frac{\delta\sqrt{R'}}{0.764}\right)^{2/3}$

Subscript:

cr indicates conditions just before transition from laminar to turbulent flow.

TEST METHODS

Models.- The tests were conducted in the Langley two-dimensional low-turbulence tunnel. The test section of this tunnel measures 3 by 7.5 feet and when mounted the models completely spanned the 3-foot dimension.

Tests were conducted with two typical laminar-flow airfoils which hereinafter will be referred to as low-drag airfoil 1 and low-drag airfoil 2. On both airfoils

the position of minimum pressure was at 0.7c; however, the pressure gradient was more favorable on low-drag airfoil 1 than on low-drag airfoil 2. Low-drag airfoil 1 was cambered for an ideal lift coefficient of 0.2 with a mean line of the type $a = 0.7$; low-drag airfoil 2 was a symmetrical section. Experimental pressure distributions are presented for the two airfoils at the given test conditions in figures 1 and 2. The models were constructed of wood and were painted and sanded to have aerodynamically smooth finishes. Each model had a chord of 90 inches.

Tests.— The projections were cylindrical and consisted of headless nails driven perpendicular into the surface until the desired height was attained. The projection heights were determined with an Ames dial gage. Tests were performed with one spanwise row of projections of constant size located at the desired chordwise station on the upper surface of the airfoil; the spanwise spacing was 3 inches in all tests. Projections of 0.035-inch diameter and various heights were employed in the tests; check tests were conducted with projections of 0.015-inch diameter. The various combinations of projection size and chordwise location tested with low-drag airfoils 1 and 2 are presented in table I. Drag data were obtained for airfoil Reynolds numbers varying from approximately 3×10^6 to 10×10^6 for the airfoils with smooth surfaces and with each combination of projection size and location. The drag measurements were made at a single spanwise location by the wake-survey method, a complete description of which appears in reference 1. For each projection combination, the Reynolds number at which the drag coefficient showed a definite increase over that of the smooth airfoil was considered to be the critical Reynolds number. The drag data were often inconclusive, particularly when the projections were located at large distances behind the leading edge. In these instances the boundary-layer transition parameter (reference 7) was determined from measurements of the velocity profile in the boundary layer. These measurements were made with a rack of total-pressure tubes (reference 7) located 2 inches behind the projections. The Reynolds number at which the boundary-layer transition parameter showed a definite increase was considered the critical value. The drag of the airfoil without projections was determined at frequent intervals to insure that all drag increments were caused by the projections and not some other surface imperfection.

Imperfect sheet-metal butt joints were simulated by grooves of several sizes cut into the surface of low-drag airfoil 1. The various combinations of groove size and configuration that were tested are presented in table II. Grooves of X-plan form are illustrated in figure 3. The procedure followed in performing the tests of the airfoil with grooves was the same as that for the airfoils with projections.

The various grades of sandpaper and carborundum paper used for determining the effects of sanding scratches on transition are indicated in table III. Not only were various grades of abrasive used to determine the effects of sanding but the direction of sanding relative to the air stream was also varied. Enlarged photographs of surface areas sanded with circular and cross-hatched strokes are shown in figure 4. The method for applying the roughness is shown in figure 5. The roughness area was progressively increased from a strip from 0.7c to 0.5c to include the part of the airfoil between 0.7c and the leading edge. Drag data were taken through the range of Reynolds number after each area was sanded.

RESULTS

Projections.- The results of the investigation of the effects of surface projections on transition are presented in figures 6 to 10. The variation of section drag coefficient with airfoil Reynolds number for the two low-drag airfoils with smooth surfaces is given in figure 6. The increase in drag coefficient for low-drag airfoil 2 at the higher airfoil Reynolds numbers is believed to have been caused by the increase in air-stream turbulence with Reynolds number. The drag of low-drag airfoil 1 was not affected by the increasing air-stream turbulence because of the more favorable pressure gradient of this airfoil. The results of the analysis given later in the discussion appear to indicate that the turbulence of the air stream had only a secondary effect on the Reynolds number at which the projections caused premature transition.

The increments of drag induced by projections of various sizes and chordwise locations are plotted against airfoil Reynolds number in figures 7 and 8. The boundary-layer transition parameter (reference 7) is plotted as a function of airfoil Reynolds number in figures 9 and 10.

Surface grooves and sanding scratches.- The results of the investigation of the effects of surface grooves and sanding scratches on transition together with the test conditions at which the results were obtained are presented in tables II and III, respectively.

DISCUSSION AND ANALYSIS

Projections.- As has already been indicated, the airfoil Reynolds number at which either the drag increment or boundary-layer transition parameter shows a definite increase is considered to be the critical Reynolds number at which premature transition occurs. The accuracy with which an increase in either of these parameters establishes the critical Reynolds number is indicated in figures 7(c) to 7(f). Several values of the critical Reynolds number were obtained with each size of projection at 0.20c on low-drag airfoil 1. The values of the critical Reynolds number obtained with each configuration generally agree within 1×10^6 . Although better agreement might be considered desirable, the results presented are thought to give a good indication of the order of magnitude of the Reynolds number at which premature transition may be expected with projections of a given size and location.

The general effects of projection size and location on transition are indicated by the experimental curves. As might be expected, the critical airfoil Reynolds number at a specified chordwise station decreases with increasing projection height and diameter. As projections of a given size are moved toward the leading edge, the critical Reynolds number decreases until the projections almost reach the stagnation point and then begins to increase. The lower critical Reynolds numbers for projections of given height at 0.65c as compared with those for projections of the same height at 0.50c (figs. 7 and 9) may be due to the combined effects of a zero or slightly unfavorable pressure gradient and larger values of the boundary-layer Reynolds number. The results obtained with projections near the stagnation point are explained by the low velocity over the surface and the steep velocity gradient at the stagnation point. The increase in critical Reynolds number as projections are placed near the stagnation point should not, however, be taken

to mean that large projections may be tolerated near the leading edge. At some angles of attack, the velocity near the leading edge would be very high and, consequently, the critical projection size small. Although the value of the critical airfoil Reynolds number varies with chordwise location of the projections, the results indicate that the critical Reynolds number is much more sensitive to variation in projection size than to variation in projection chordwise location. A comparison of the results obtained with the two low-drag airfoils indicates that the symmetrical airfoil has a higher critical Reynolds number for a given configuration than the cambered airfoil. This result is quite reasonable since the local velocity over the upper surface is higher for the cambered section than for the symmetrical section and the boundary layer is therefore thinner.

The manner in which the drag coefficient varies with airfoil Reynolds number depends on the way in which premature transition occurs. The movement of the transition point from its original position to the position of the disturbance may extend over a considerable range of Reynolds number. This process occurs as a result of an unsteadiness or waviness induced in the boundary layer that grows in amplitude as the distance behind the disturbing element is increased. If the original length of laminar flow is sufficiently great, the unsteadiness induced by the disturbance will increase to such a degree as to cause premature transition before the original transition point is reached (references 8 and 9). As the Reynolds number increases, the position of critical unsteadiness moves forward and causes a progressive decrease in the extent of laminar flow in the boundary layer so that the drag shows a gradual increase over a considerable range of airfoil Reynolds number.

In the present tests, however, (figs. 7 to 10) the transition point seems to move, at a particular value of the airfoil Reynolds number, abruptly forward from its original position. In some of the figures, the value of the drag rises abruptly and then continues to rise with increasing Reynolds number but more slowly than before. The ultimate value of the drag corresponds presumably to transition at the projection. The continued rise in drag after the first abrupt increase may indicate either that the transition point did not necessarily move all the way to the disturbance as soon as the critical Reynolds number was exceeded or that all the projections in the single

spanwise row across the airfoil did not have exactly the same height and shape and therefore the same critical Reynolds number. In any case, the sharp rise in drag seems characteristic of the projections tested.

An attempt was made to correlate the critical airfoil Reynolds numbers at which the projections caused premature transition with local-flow conditions around the projection (reference 10). In such an analysis of the results, certain variables are neglected, such as tunnel turbulence, pressure gradient, boundary-layer Reynolds number, and the original extent of laminar flow, except insofar as these variables affect local-flow conditions.

Similarity of local-flow conditions about projections in similar fields of flow is obtained if the projections are geometrically similar and if the Reynolds number of the flow about the projections is the same. In the following analysis, the projections are taken to be sufficiently small to make $\partial u/\partial y$ in the absence of the projection essentially constant from the surface to a height equal to the height of the projection. Cylindrical projections are geometrically similar if their fineness ratios d/k are the same. For each value of d/k the local-flow pattern is therefore completely determined by the Reynolds number of the flow about the projection. The Reynolds number of the flow about the projection R_k was taken to be $\frac{u_k k}{\nu}$. The critical projection Reynolds number $R_{k_{cr}}$ was calculated from the experimental data corresponding to the critical airfoil Reynolds number as indicated by the curves of figures 7 to 10. The Blasius relation for $\partial u/\partial y$, expressed in terms of the boundary-layer thickness was employed for calculating u_k . The variation of the boundary-layer thickness with chordwise position at Reynolds numbers of 3×10^6 and 9×10^6 is given in figure 11 for low-drag airfoils 1 and 2. The boundary-layer thicknesses were calculated by means of equation (B1) of appendix B. The final equation for the critical projection Reynolds number is as follows:

$$R_{k_{cr}} = 0.764 \left(\frac{k}{\delta_{cr}} \right)^2 R_{\delta_{cr}} \quad (1)$$

██████████

The derivation of equation (1) is given in appendix A and the method of reducing the experimental data to obtain $R_{k_{cr}}$ is outlined in appendix B.

Values of $\sqrt{R_{k_{cr}}}$ are plotted against the corresponding values of the projection fineness ratio d/k in figure 12. In this figure $\sqrt{R_{k_{cr}}}$ was used as a variable rather than $R_{k_{cr}}$ because $\sqrt{R_{k_{cr}}}$ is directly proportional to the critical projection height.

The considerable scatter of the points shown in figure 12 appears to be unsystematic. The scatter may have been caused primarily either by the neglect of some of the variables previously mentioned or by experimental inaccuracies in determining the critical airfoil Reynolds number for a given projection. Check tests of the critical Reynolds number have been shown to differ by approximately 1×10^6 . In order to indicate the practical significance of the scatter of the data shown in figure 12, curves of projection height against critical airfoil Reynolds number have been calculated from the faired curve of figure 12 by means of the relation presented in appendix C. The comparison of the experimental points with the calculated curves (figs. 13 and 14) shows that virtually all the experimental points of the critical Reynolds number can be made to agree with the calculated curves by shifting the points not more than 0.5×10^6 on the Reynolds number scale and not more than 0.002 inch on the height scale. The results therefore indicate that, with the exception of the points obtained for projections close to the stagnation point, the effects of small projections on transition can be correlated with local-flow conditions within the limits of experimental error in this investigation.

The data from which $\sqrt{R_{k_{cr}}}$ was correlated with d/k were taken at Reynolds numbers from approximately 3×10^6 to 10×10^6 . It is reasonable to believe, however, that the correlation would be valid at higher Reynolds numbers. A consideration of the parameters describing the boundary layer indicates that conditions near the leading edge at high Reynolds numbers are equivalent to conditions farther back at low Reynolds numbers. The analysis presented is then particularly applicable when small values of x/c

are considered with relation to high Reynolds numbers. Inasmuch as all tests were made with one spanwise row of cylindrical projections, the critical Reynolds number may be somewhat optimistic for projections likely to occur in practice because of variations in the shape of the projections from the type investigated and possible combined effects of a number of projections at various chordwise locations. It should also be noted that the analysis was based on data in which the height of the projection was small compared to the boundary-layer thickness and can be expected to apply only when this condition is fulfilled.

Page has presented the results of experiments conducted for the purpose of determining a criterion for the critical height of either a single arch or a flat ridge located in a spanwise direction at various chordwise positions on a low-drag airfoil (reference 3) and a flat plate (reference 4). The criterion as determined from the airfoil tests was presented in the form of a correlation of $R_{k_{cr}}$ with k/c , where c is the airfoil chord and k the ridge height. The values of $R_{k_{cr}}$ determined from the flat-plate tests were correlated with k/L , where L is the original length of laminar flow. Although the drag data presented in reference 3 show that the critical Reynolds number is somewhat dependent upon the design length of laminar flow, the values of $\sqrt{R_{k_{cr}}}$ determined from these two investigations were plotted in figure 15 as a function of d/k , where d , in this case, was taken to be the ridge width. The parameter d/k is similar to the projection fineness ratio in that it describes the form or geometry of the boundary-layer disturbance. The values of $\sqrt{R_{k_{cr}}}$ obtained from tests made with projections and ridges are not strictly comparable, since ridges represent a two-dimensional disturbance and projections are three-dimensional. Values of $R_{k_{cr}}$ obtained from the investigation of three-dimensional projections are, however, also included in figure 15 and show the similarity between the results obtained with the two distinctive types of disturbance. Although the values of $\sqrt{R_{k_{cr}}}$ obtained with the two types of disturbance do not form a continuous curve, they are of the same order of magnitude.

In order to check Page's results, a strip of "Scotch" cellulose tape simulating a spanwise ridge was applied to low-drag airfoil 1. Two thicknesses were employed and the results, which are plotted in figure 15, are in fair agreement with Page's results. Page also made tests with a spanwise wire located at various chordwise positions (reference 3). Wires of three diameters were tested; the value of d/k was, of course, 1 in all cases. The values of $\sqrt{R_{k_{cr}}}$ obtained were 13.1, 13.5, and 8.6. Tani, Hama, and Mituisi (reference 6) conducted similar tests with wires located on an airfoil and a flat plate. The values of $\sqrt{R_{k_{cr}}}$ were 13 for a flat plate and 15 for an airfoil.

Surface grooves and sanding scratches.— The results of the investigation of the effects of surface grooves and sanding scratches indicate that within the range of Reynolds number from 3×10^6 to 10×10^6 , at which these tests were conducted, the boundary layer is relatively insensitive to surface scratches. Only deep X-plan-form grooves located near the leading edge caused premature transition (table II). No definite indications of premature transition were noticed with any of the types of sanded surface. The drag was somewhat high when the surface was finished with No. $1\frac{1}{2}$ sandpaper, but there was no definite break in the drag curve. It is thought that at higher Reynolds numbers than those at which the tests were made the type of sanded surface would show a more definite effect upon transition. A comparison of the results obtained with various types of surface imperfections indicates clearly that, within a given range of Reynolds number, the laminar boundary layer is much more sensitive to surface projections than to indentations in the surface.

CONCLUSIONS

From tests conducted with two typical low-drag airfoils of 90-inch chord to determine the effects of surface projections, grooves, and sanding scratches on boundary-layer transition, the following conclusions were reached:

1. The Reynolds number at which one row of spanwise projections causes premature transition is primarily a

function of the projection geometry and the Reynolds number based on the height of the projection and the velocity at the top of the projection, provided the height of the projection is small compared with the boundary-layer thickness.

2. The laminar boundary layer is more sensitive to surface projections than to surface grooves or sanding scratches.

Langley Memorial Aeronautical Laboratory
National Advisory Committee for Aeronautics
Langley Field, Va.

[REDACTED]

APPENDIX A

$$\text{DERIVATION OF } R_{k_{cr}} = 0.764 \left(\frac{k}{\delta_{cr}} \right)^2 R_{\delta_{cr}}$$

The parameter R_k may be thought of as a Reynolds number based on the projection height and the boundary-layer velocity at the top of the projection; that is,

$$R_k = \frac{uk}{v}$$

For small values of y , the velocity u in the laminar boundary layer may be expressed as a linear function of y by

$$u = y \frac{du}{dy}$$

then

$$u_k = k \frac{du}{dy}$$

so that

$$R_k = \frac{k^2}{v} \frac{du}{dy}$$

In order that R_k may be more easily calculated, the Blasius relation (reference 11) for the slope of the laminar boundary-layer velocity profile is introduced

$$\frac{du}{dy} = 0.332 \frac{U}{x} \sqrt{R_x} \quad (A2)$$

The substitution of equation (A2) into the expression for the projection Reynolds number gives

$$R_k = k^2 0.332 \frac{U}{v} \frac{\sqrt{R_x}}{x} \quad (A3)$$

The Blasius expression (reference 11) for the boundary-layer thickness, which is defined as the distance normal to the wing surface at which $\frac{u}{U} = 0.707$, is

$$\delta = \frac{2.3x}{\sqrt{R_x}}$$

Since in equation (A3) δ

$$\frac{\sqrt{R_x}}{x} = \frac{2.3}{\delta}$$

equation (A3) may be written as

$$R_k = 0.764 \frac{k^2}{\delta} \frac{U}{\nu}$$

but

$$\frac{U}{\nu} = R'$$

therefore

$$R_k = 0.764 \frac{k^2}{\delta} R'$$

If the numerator and denominator are multiplied by δ

$$R_k = 0.764 \left(\frac{k}{\delta} \right)^2 R_\delta \quad (A4)$$

If δ is taken as the boundary-layer thickness just before transition from laminar to turbulent flow, then R_δ is the critical boundary-layer Reynolds number and equation (A4) may be written as follows:

$$R_{k_{cr}} = 0.764 \left(\frac{k}{\delta_{cr}} \right)^2 R_{\delta_{cr}} \quad (A5)$$

APPENDIX B

DETERMINATION OF $R_{k_{cr}}$ FROM EXPERIMENTAL DATA

From equation (A5), it is seen that the values of R_δ and δ which correspond to the airfoil Reynolds number at transition must be calculated. A suitable equation for δ is obtained by assuming a Blasius velocity distribution and integrating the von Kármán momentum relation. The following equation results (reference 12):

$$\delta^2 = 5.3 \frac{c v}{U} \left(\frac{U_0}{U} \right)^{8.17} \int_0^{s/c} \left(\frac{U}{U_0} \right)^{8.17} d \frac{s}{c} \quad (B1)$$

A more convenient relation is obtained if equation (B1) is multiplied by R'

$$(\delta \sqrt{R'})^2 = 5.3 c \left(\frac{U_0}{U} \right)^{8.17} \int_0^{s/c} \left(\frac{U}{U_0} \right)^{8.17} d \frac{s}{c} \quad (B2)$$

The numerical value of equation (B2) is a constant for any chordwise position and need be calculated only once for each position at which tests are being conducted. The critical values of δ and R_δ may be calculated from equation (B2) when the critical Reynolds number R_{cr} has been experimentally determined. By definition,

$$R' = \frac{U}{v}$$

but

$$R_{cr} = \frac{U_0 c}{v}$$

therefore,

$$R' = \frac{U}{U_0 c} R_{cr} \quad (B3)$$

The boundary-layer thickness is then obtained by dividing the square root of R' , as determined from equation (B3), into the constant $\delta \sqrt{R'}$. In order to obtain R_δ , it is only necessary to multiply δ by R' . All the variables in equation (A5) are now known, and $R_{k_{cr}}$ may be calculated.

APPENDIX C

$$\text{DERIVATION OF } R_{cr} = A \left(\frac{\sqrt{R_{k_{cr}}}}{k} \right)^{1.333}$$

Since

$$R_{k_{cr}} = 0.764 \left(\frac{k}{\delta_{cr}} \right)^2 R \delta_{cr}$$

then

$$\frac{R_{k_{cr}}}{k^2 0.764} = \frac{R'_{cr}}{\delta_{cr}} \quad (C1)$$

If both sides of equation (B1) are multiplied by $\delta_{cr} \sqrt{R'_{cr} c}^{3/2} \left(\frac{U_o}{U} \right)^{3/2}$

$$\left(\frac{U_o}{U} \right)^{3/2} \frac{\delta_{cr} \sqrt{R'_{cr} c}^{3/2} R_{k_{cr}}}{0.764 k^2} = \left(\frac{U_o}{U} \right)^{3/2} R'_{cr} c^{3/2} = R_{cr} c^{3/2}$$

but $\frac{U_o}{U} \delta_{cr} \sqrt{R'_{cr}}$ is constant for any given chordwise position so that

$$R_{cr} = A \left(\frac{R_{k_{cr}}}{k^2} \right)^{2/3} = A \left(\frac{\sqrt{R_{k_{cr}}}}{k} \right)^{1.333}$$

where

$$A = \frac{U_o c}{U} \left(\frac{\delta_{cr} \sqrt{R'_{cr}}}{0.764} \right)^{2/3}$$

REFERENCES

1. Abbott, Ira H., von Doenhoff, Albert E., and Stivers, Louis S., Jr.: Summary of Airfoil Data. NACA ACR No. L5C05, 1945.
2. Abbott, Frank T., Jr., and Turner, Harold R., Jr.: The Effects of Roughness at High Reynolds Numbers on the Lift and Drag Characteristics of Three Thick Airfoils. NACA ACR No. L4E21, 1944.
3. Fage, A.: The Effect of Narrow Spanwise Surface Ridges on the Drag of a Laminar-Flow Aerofoil. 5950, Ae. 2019, British A.R.C., July 13, 1942.
4. Fage, A.: The Effect of Narrow Spanwise Surface Ridges on the Drag of a Laminar-Flow Aerofoil. 6126, Ae. 2019a, British A.R.C., Sept. 22, 1942.
5. Fage, A.: The Smallest Size of a Surface Bulge, a Ridge or Hollow, Which Affects the Drag of a Laminar-Flow Aerofoil. 6443, Ae. 2148, British A.R.C., Jan. 22, 1943.
6. Tani, Itiro, Hama, Ryosuke, and Mituisi, Satosi: On the Permissible Roughness in the Laminar Boundary Layer. Rep. No. 199 (vol. XV, 13), Aero. Res. Inst., Tokyo Imperial Univ., Oct. 1940.
7. von Doenhoff, Albert E.: Investigation of the Boundary Layer about a Symmetrical Airfoil in a Wind Tunnel of Low Turbulence. NACA ACR, Aug. 1940.
8. Schubauer, G. B., and Skramstad, H. K.: Laminar-Boundary-Layer Oscillations and Transition on a Flat Plate. NACA ACR, April 1943.
9. Tollmien, W.: The Production of Turbulence. NACA TM No. 609, 1931.
10. Schiller, L.: Strömung in Röhren. Handbuch der Experimentalphysik; Bd. IV, 4. Teil, Hydro- und Aerodynamik; Ludwig Schiller, Hrsg.; Akad. Verlagsgesellschaft m. b. H. (Leipzig), 1932, p. 191.

11. Prandtl, L.: The Mechanics of Viscous Fluids. The Flat Plate. Vol. III of Aerodynamic Theory, div. G, sec. 11, W. F. Durand, ed., Julius Springer (Berlin), 1935, pp. 84-90.
 12. Jacobs, E. N., and von Doenhoff, A. E.: Formulas for Use in Boundary-Layer Calculations on Low- Drag Wings. NACA ACR, Aug. 1941.
- ████████████████████

TABLE I

COMBINATIONS OF SIZE AND CHORDWISE LOCATION OF PROJECTIONS
TESTED WITH LOW-DRAG AIRFOILS 1 AND 2

Low-drag airfoil 1			Low-drag airfoil 2		
Chordwise location	Diam. (in.)	Height (in.)	Chordwise location	Diam. (in.)	Height (in.)
0.0007c .0007c .0007c	0.035 .035 .035	0.04 .06 .08	0.05c .05c .05c .05c .05c	0.035 .035 .035 .035 .035	0.010 .015 .020 .025 .030
0.058c .058c .058c	0.035 .035 .035	0.005 .010 .015	0.20c .20c .20c .20c .20c .20c .20c .20c .20c .20c .20c	0.035 .035 .035 .035 .035 .035 .035 .035 .035 .035 .035	0.010 .011 .012 .015 .020 .025 .030 .035 .040 .050
0.20c .20c .20c .20c .20c	0.035 .035 .035 .035 .035	0.009 .015 .020 .024 .025	0.20c .20c .20c .20c .20c .20c .20c .20c .20c .20c .20c	0.015 .015 .015 .015 .015 .015 .015 .015 .015 .015 .015	0.013 .014 .015 .016 .018 .019 .021 .023 .025
0.35c .35c .35c .35c	0.035 .035 .035 .035	0.010 .015 .020 .025	0.50c .50c .50c .50c .50c	0.035 .035 .035 .035 .035	0.010 .015 .020 .025 .030 .040
0.50c .50c .50c .50c .50c	0.035 .035 .035 .035 .035	0.010 .015 .025 .030 .035 .040 .045	0.65c .65c .65c .65c .65c .65c .65c .65c	0.035 .035 .035 .035 .035 .035 .035 .035	0.010 .015 .020 .025 .030 .035 .040 .050

TABLE II

EFFECTS OF UPPER-SURFACE GROOVES ON DRAG CHARACTERISTICS
OF LOW-DRAG AIRFOIL 1

Groove description	Remarks
Spanwise groove 0.005 in. deep and 0.005 in. wide at 0.20c	No measurable increase in drag over that of smooth wing for range of Reynolds number from 3×10^6 to 10.57×10^6 .
Spanwise groove 0.008 in. deep and 0.010 in. wide at 0.20c	Do.
Spanwise grooves 0.008 in. deep and 0.010 in. wide at 0.20c and 0.058c	Do.
Spanwise grooves 0.008 in. deep and 0.010 in. wide at 0.20c, 0.058c, and 0.00c	Do.
Spanwise groove 0.009 in. deep and 0.013 in. wide at 0.058c	Do.
Spanwise groove 0.009 in. deep and 0.021 in. wide at 0.058c	Do.
Grooves 0.030 in. deep and 0.05 in. wide in X-plan form at approx. 0.050c (see fig. 3)	Premature transition indicated by sudden increase in drag at a Reynolds number of 6.95×10^6 .

TABLE III

SUMMARY OF DRAG RESULTS FROM TESTS OF LOW-DRAG AIRFOIL 1
FINISHED WITH VARIOUS GRADES OF SANDPAPER
AND CARBORUNDUM PAPER

[All tests were made of low-drag airfoil 1 at Reynolds numbers from approximately 3×10^6 to 10.57×10^6]

Abrasive	Chordwise extent of roughness	Sanding strokes	Effect on drag
No. 320 carborundum paper	0.7c to 0.0c sanded in steps as indicated in figure 5	Parallel to wind direction	No measurable increase in drag over that of smooth wing
No. 320 carborundum paper	-----do-----	Perpendicular to wind direction	Do.
No. 320 carborundum paper	-----do-----	45° to wind direction	Do.
No. 280 carborundum paper	-----do-----	Parallel to wind direction	Do.
No. 280 carborundum paper	-----do-----	Perpendicular to wind direction	Do.
No. 280 carborundum paper	Complete surface	Erratic	Do.

TABLE III - Concluded

SUMMARY OF DRAG RESULTS FROM TESTS - Concluded

Abrasive	Chordwise extent of roughness	Sanding strokes	Effect on drag
No. 180 carborundum paper	Complete surface	Erratic	No measurable increase in drag over that of smooth wing
No. 120 carborundum paper	-----do-----	Cross-hatched (see fig. 4)	Do.
No. 120 carborundum paper	-----do-----	Circular (see fig. 4)	Do.
No. $1\frac{1}{2}$ sandpaper	0.7c to 0.3c	Perpendicular to wind direction	Drag slightly high at Reynolds number of 10.57×10^6
No. $1\frac{1}{2}$ sandpaper .	-----do-----	Erratic	Do.

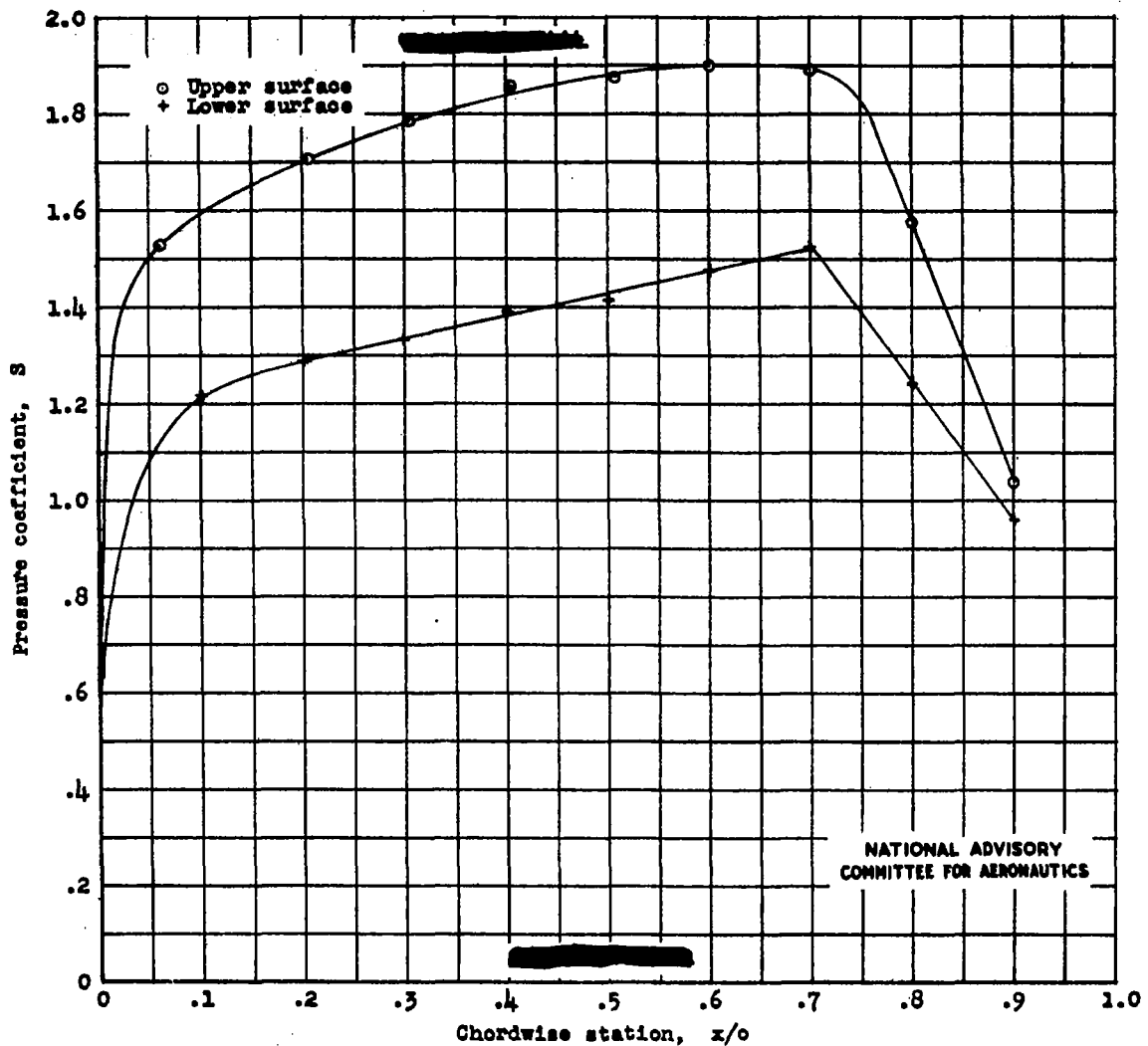


Figure 1 .- Pressure distribution of low-drag airfoil 1 at a lift coefficient of 0.347.

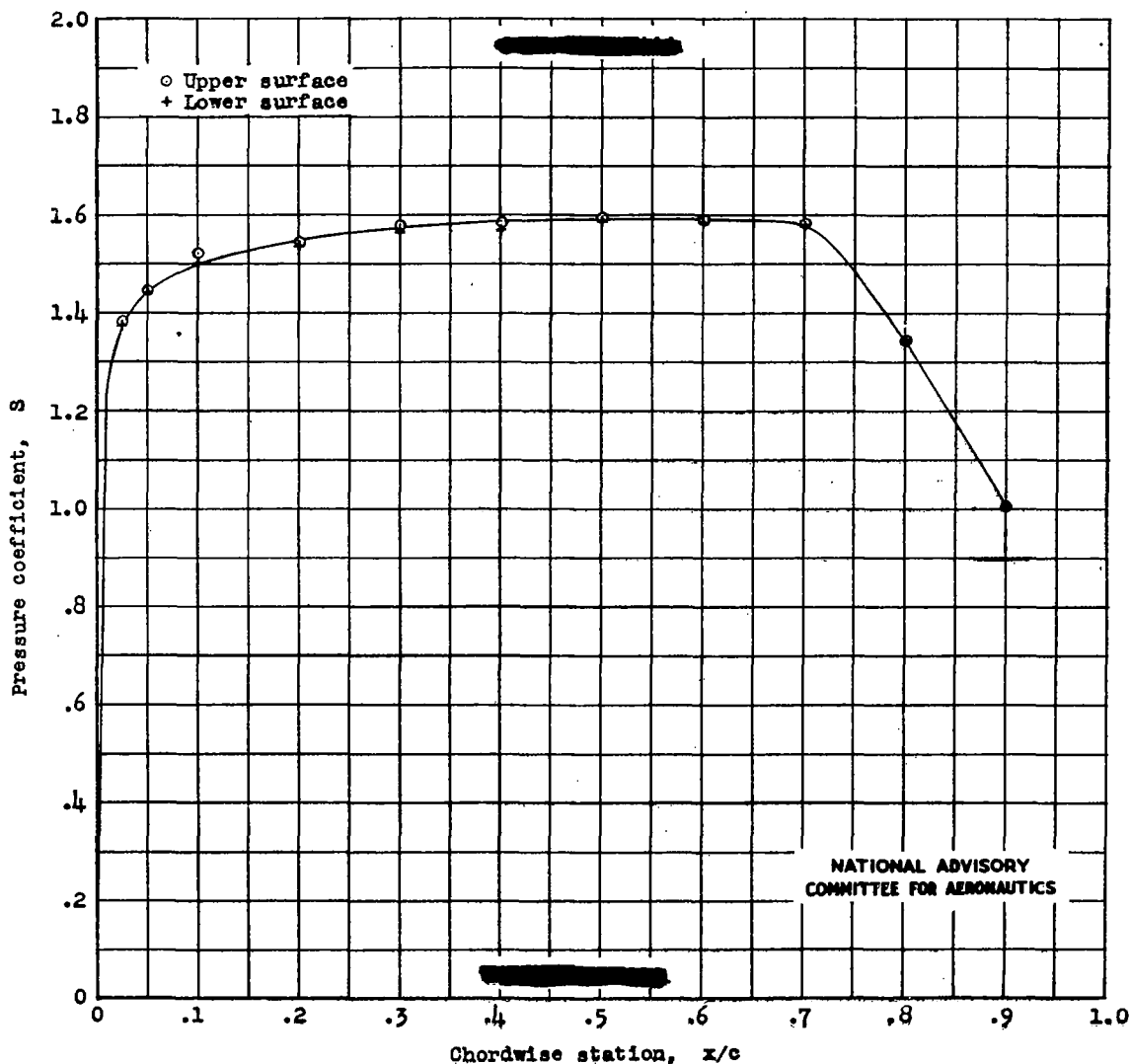
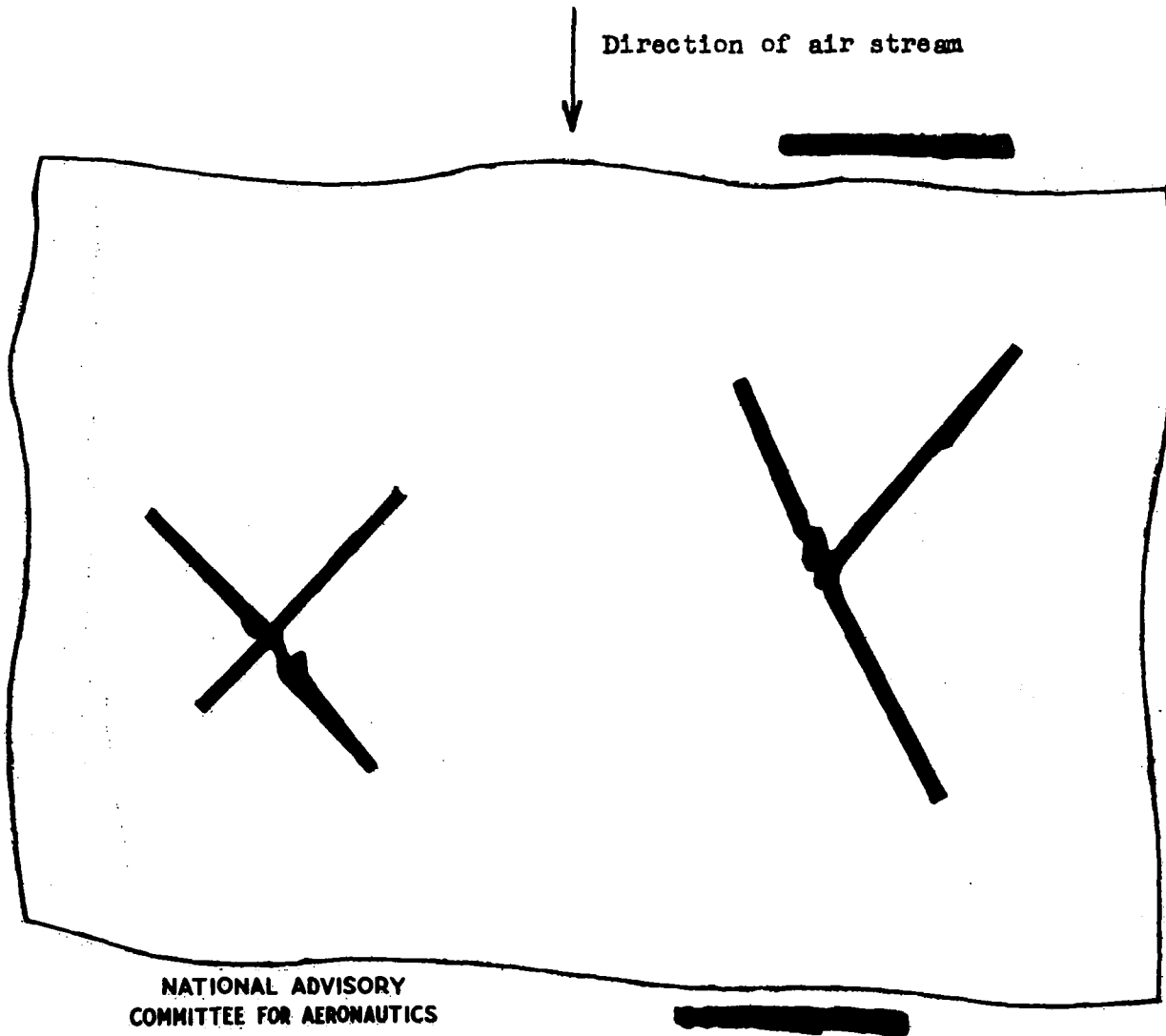
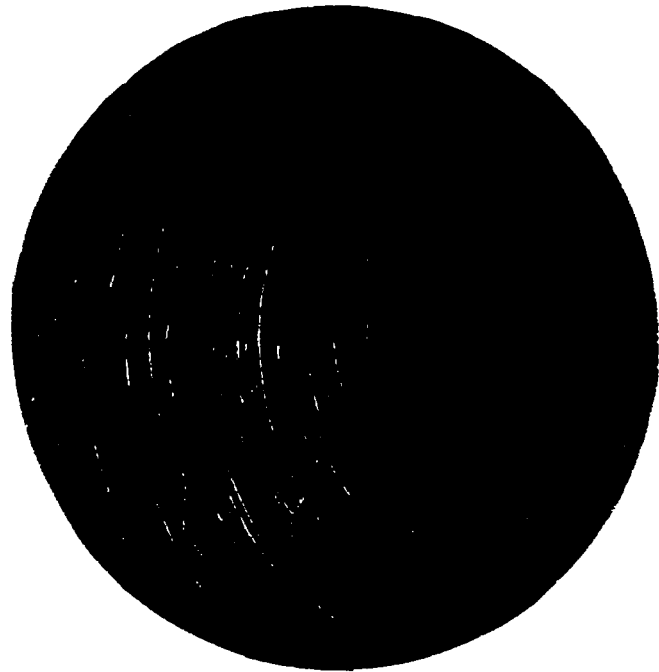


Figure 2 .- Pressure distribution of low-drag airfoil 2 at a lift coefficient of 0.



NATIONAL ADVISORY
COMMITTEE FOR AERONAUTICS

Figure 3 .- Grooves of X-plan form 0.030 inch deep and 0.050 inch wide at 0.05c on low-drag airfoil 1.



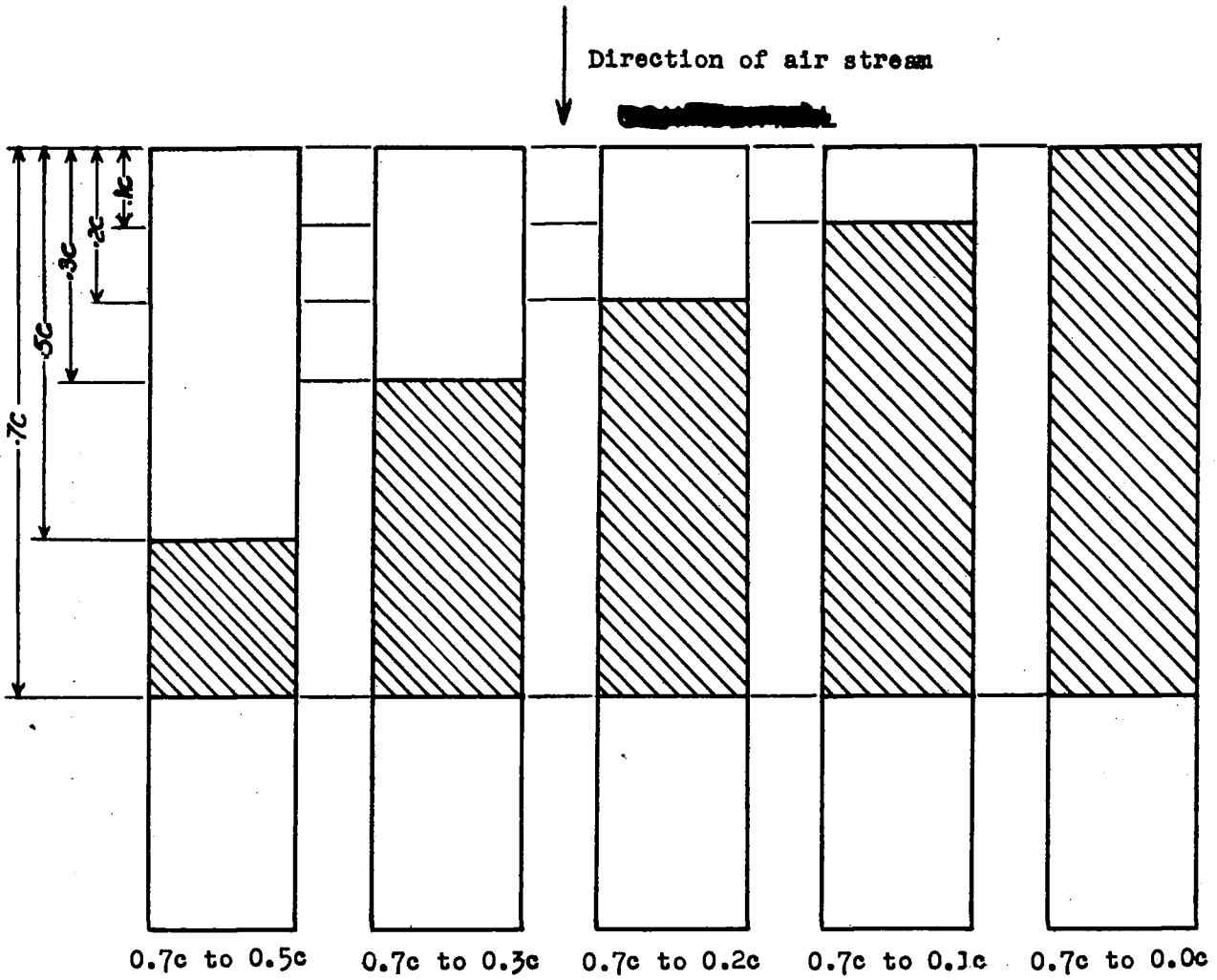
(a) Circular strokes.



(b) Cross-hatched strokes.

NATIONAL ADVISORY
COMMITTEE FOR AERONAUTICS

Figure 4.- Enlarged photographs of wing surface sanded with circular and cross-hatched strokes.



0.7c to 0.5c 0.7c to 0.3c 0.7c to 0.2c 0.7c to 0.1c 0.7c to 0.0c

NATIONAL ADVISORY
COMMITTEE FOR AERONAUTICS

Figure 5.- Plan views of wing showing progressive areas of sanding from 0.7c to 0.0c.

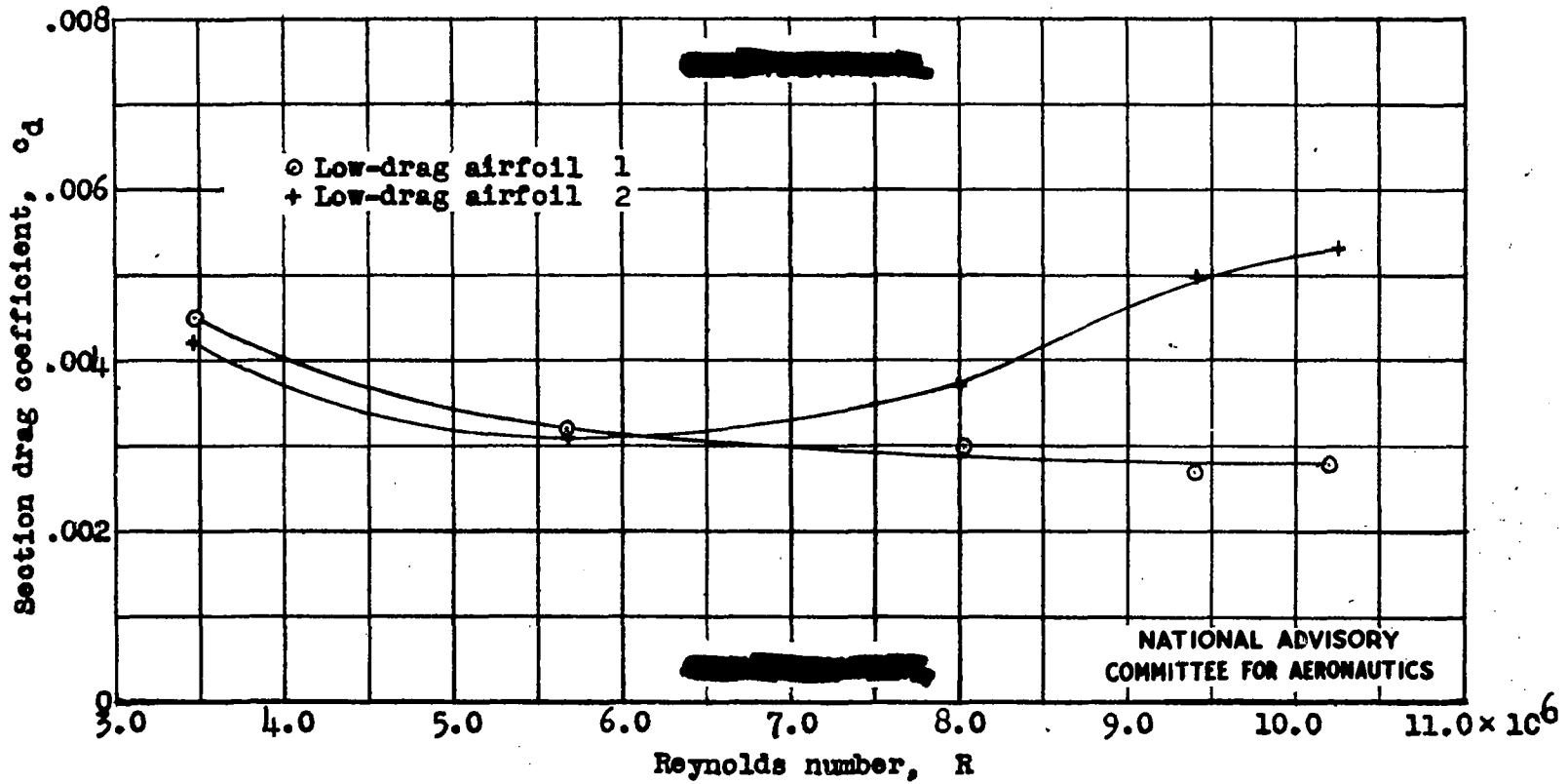
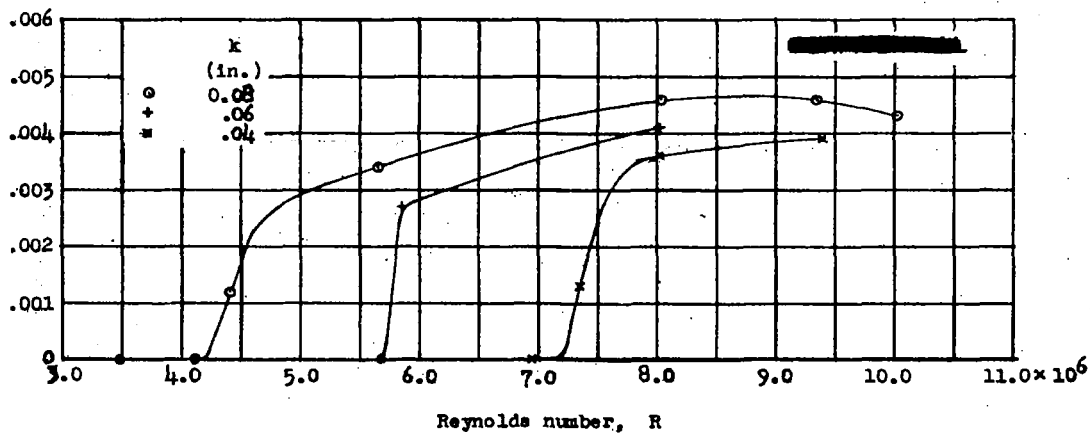
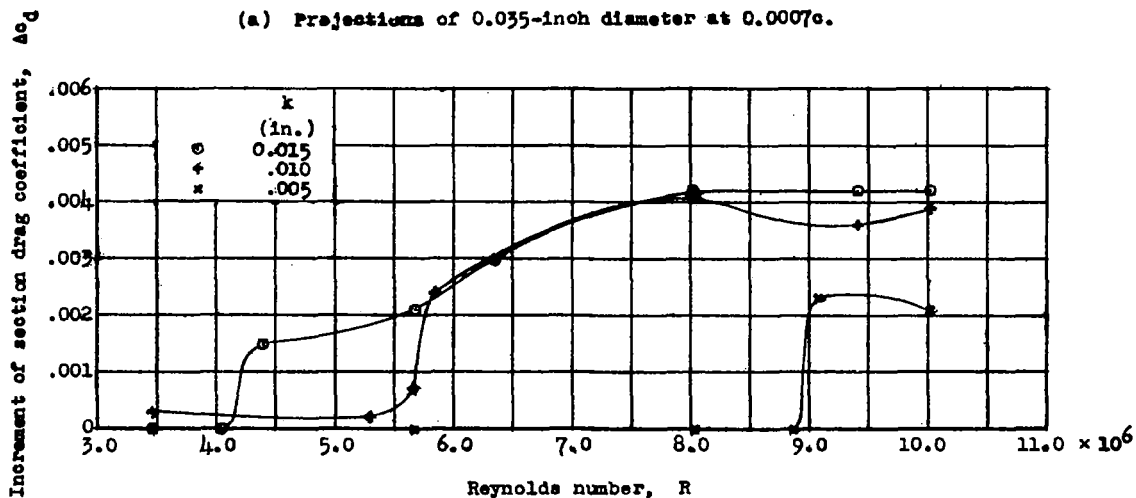


Figure 6 .- Variation of section drag coefficient with Reynolds number for low-drag airfoils 1 and 2 with smooth surfaces.

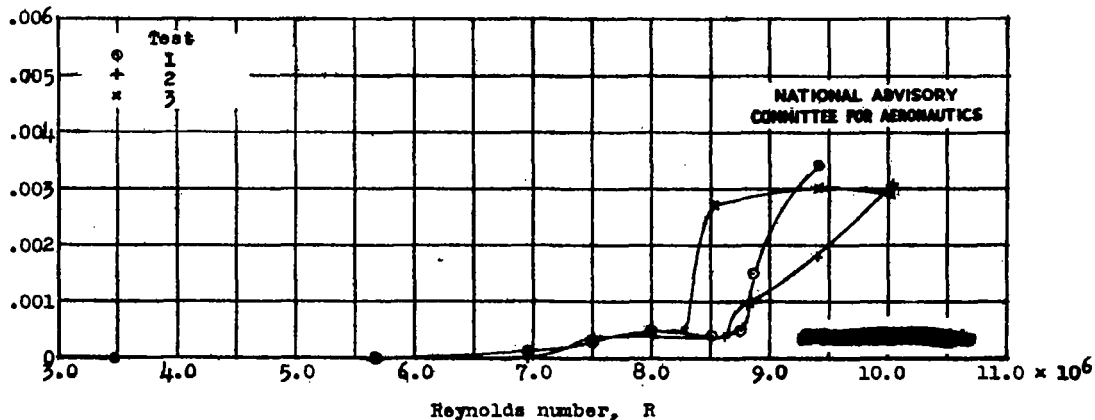
NATIONAL ADVISORY
COMMITTEE FOR AERONAUTICS



(a) Projections of 0.035-inch diameter at 0.0007c.

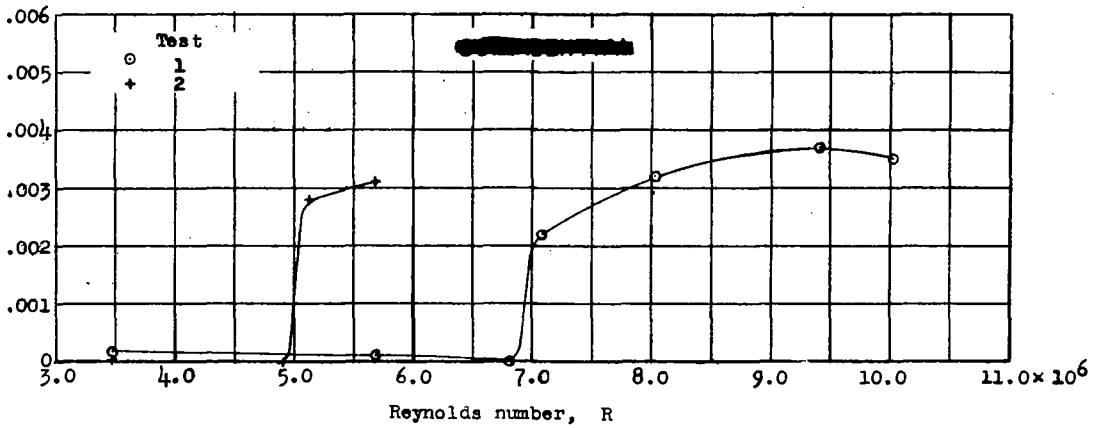


(b) Projections of 0.035-inch diameter at 0.058c.

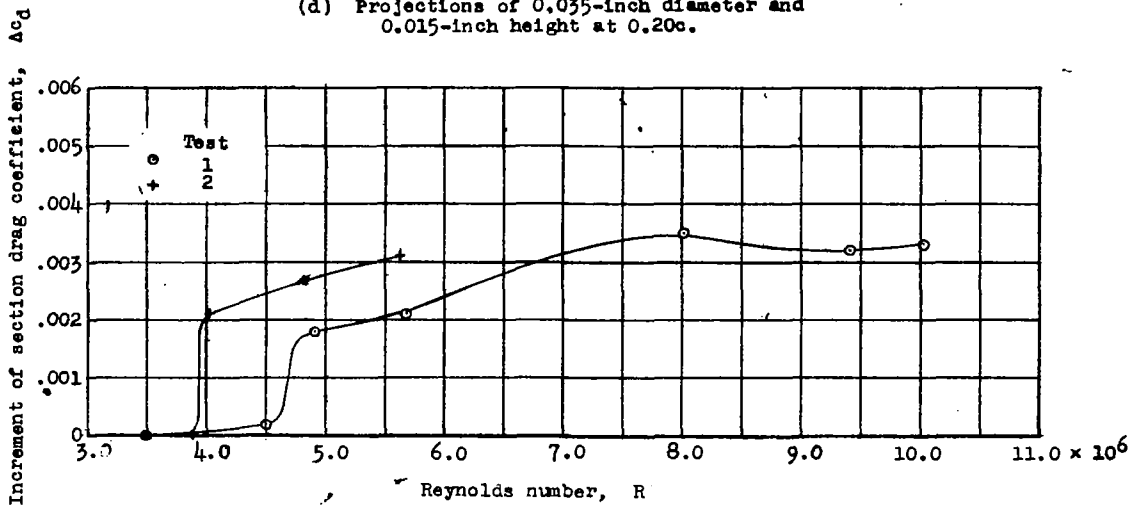


(c) Projections of 0.035-inch diameter and 0.009-inch height at 0.20c.

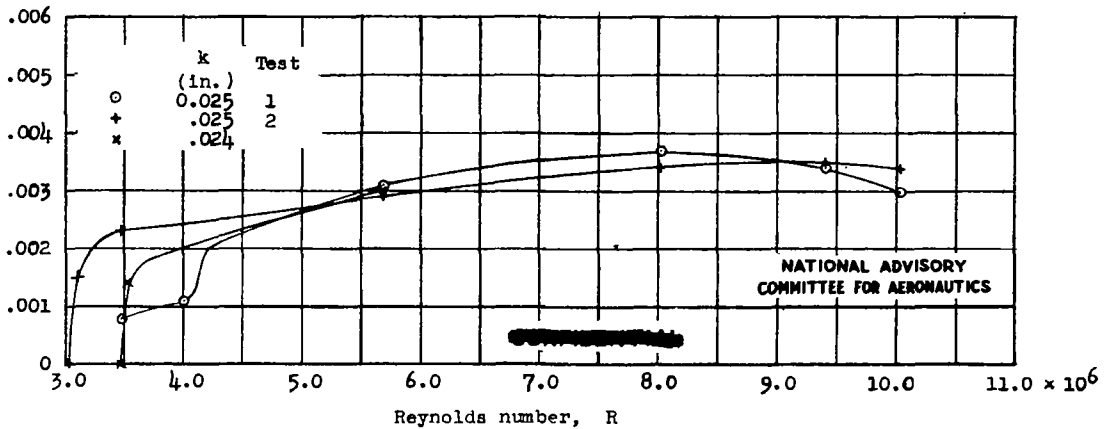
Figure 7.- Increment of section drag coefficient as a function of Reynolds number for projections of various sizes and chordwise locations on low-drag airfoil 1.



(d) Projections of 0.035-inch diameter and 0.015-inch height at 0.20c.

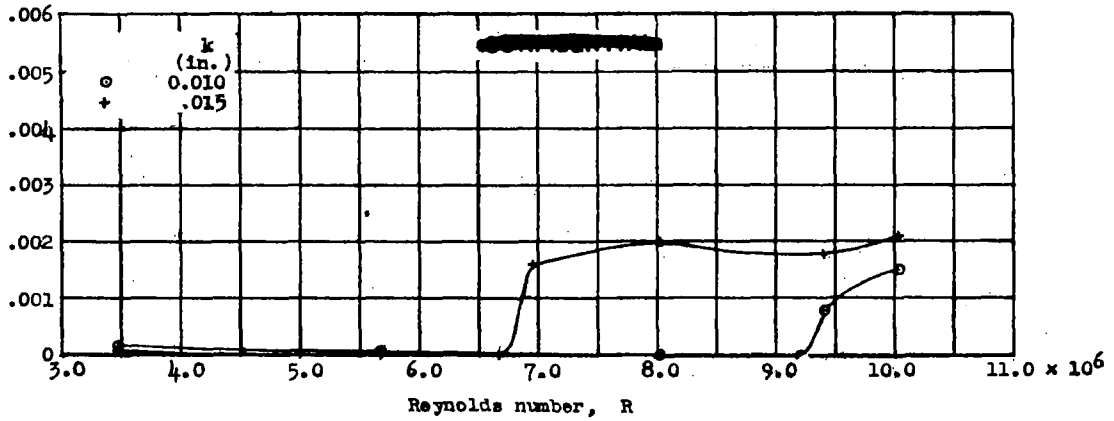


(e) Projections of 0.035-inch diameter and 0.020-inch height at 0.20c.

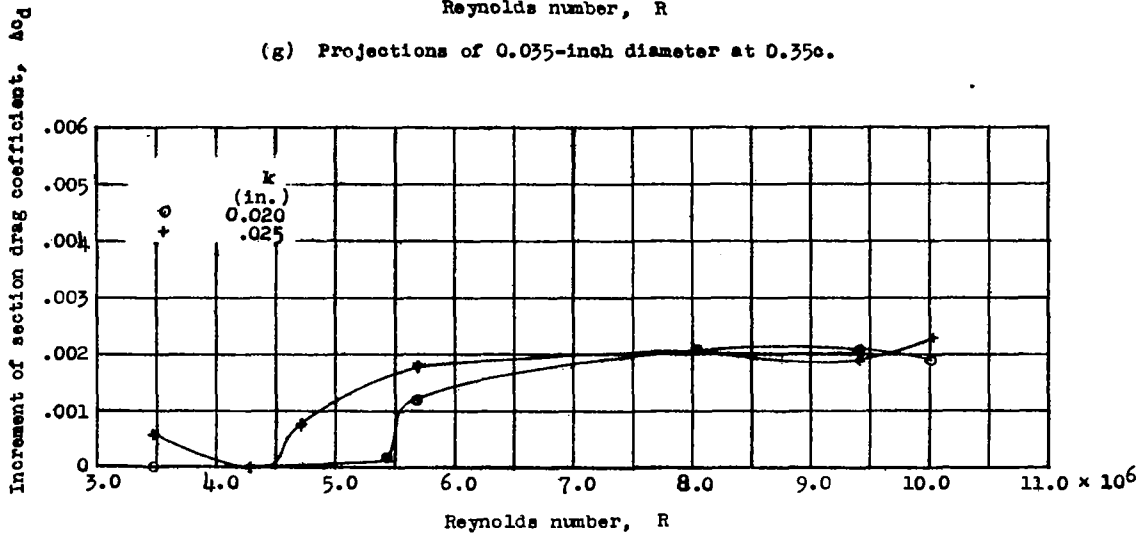


(f) Projections of 0.035-inch diameter at 0.20c.

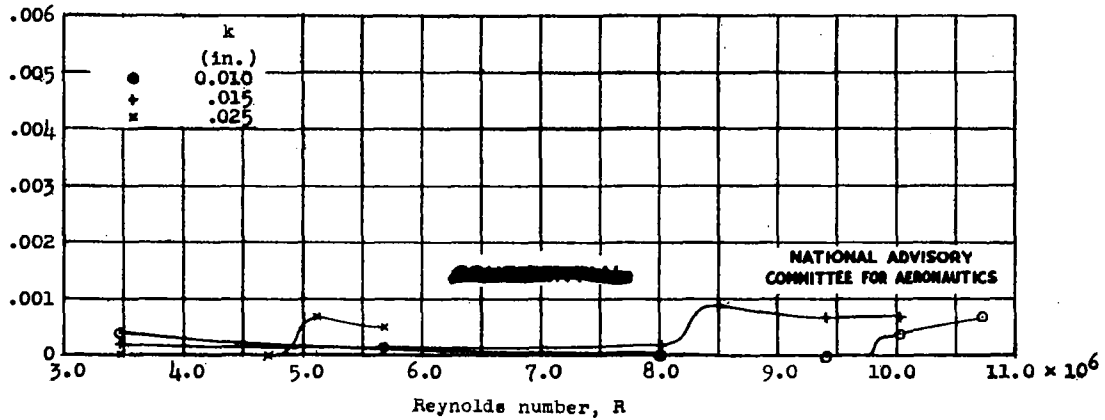
NATIONAL ADVISORY
COMMITTEE FOR AERONAUTICS



(g) Projections of 0.035-inch diameter at 0.35c.



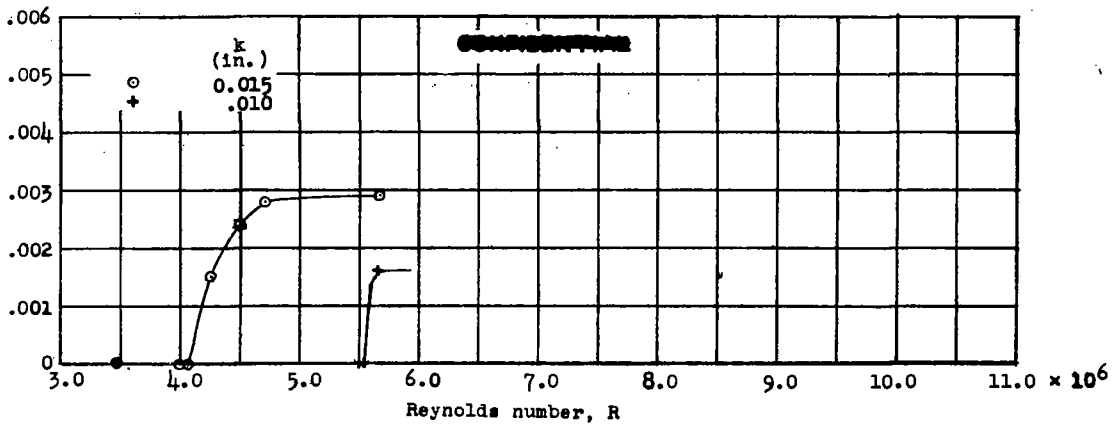
(h) Projections of 0.035-inch diameter at 0.35c.



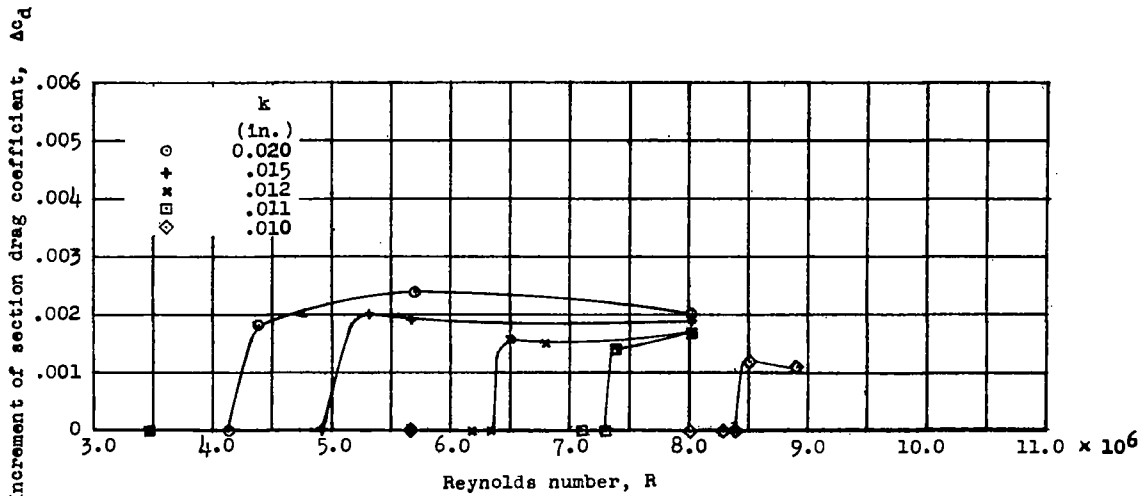
(i) Projections of 0.035-inch diameter at 0.50c.

Figure 7.- Concluded.

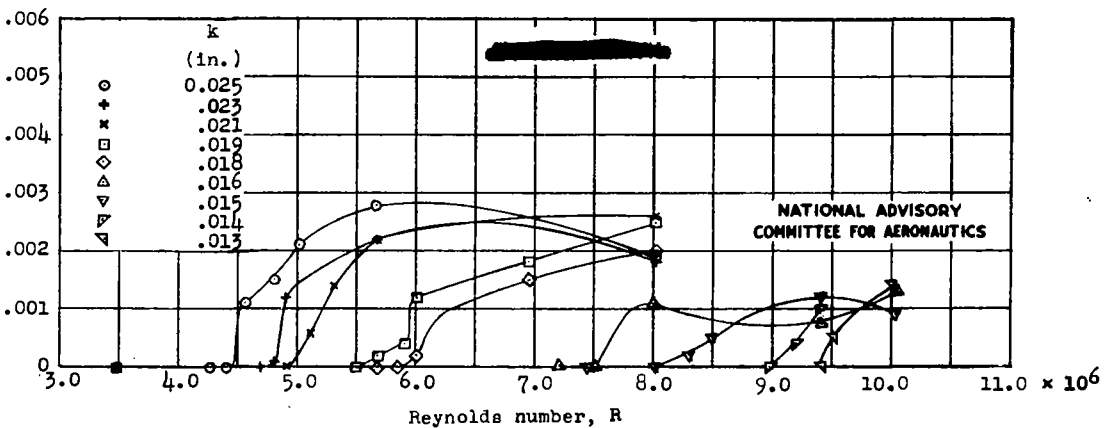
NATIONAL ADVISORY
 COMMITTEE FOR AERONAUTICS



(a) Projections of 0.035-inch diameter at 0.05c.

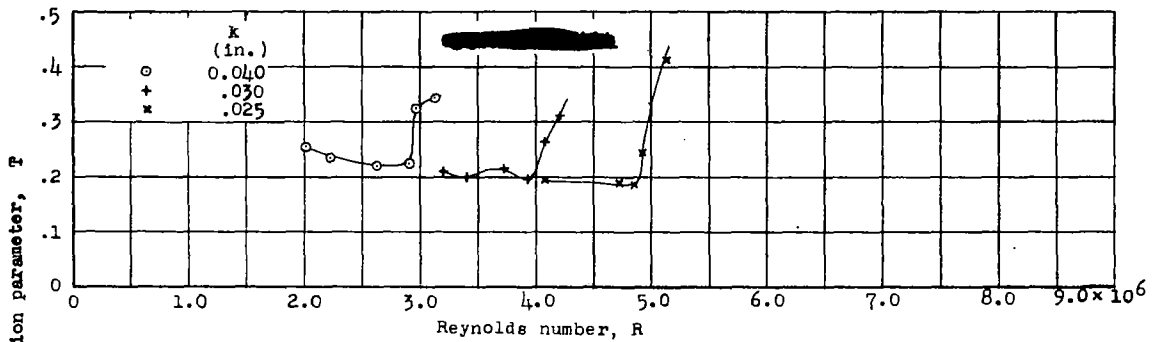


(b) Projections of 0.035-inch diameter at 0.20c.

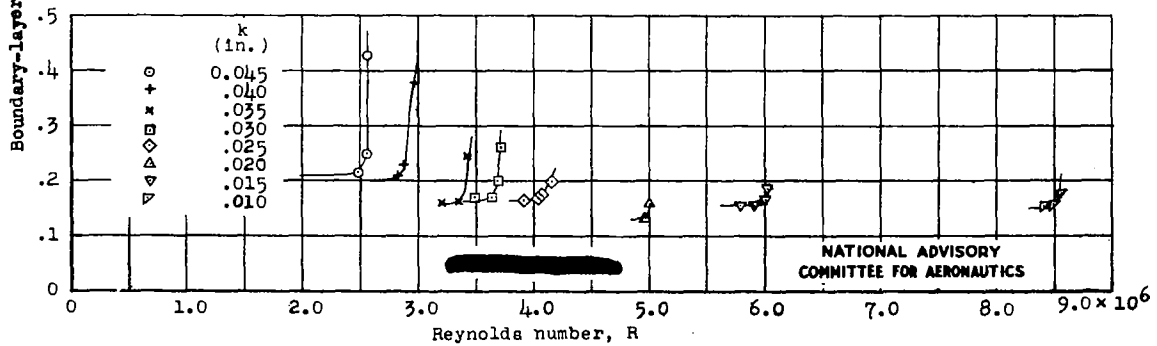


(c) Projections of 0.015-inch diameter at 0.20c.

Figure 8.- Increment of section drag coefficient as a function of Reynolds number for projections of various sizes and chordwise locations on low-drag airfoil 2.



(a) Projections of 0.035-inch diameter at 0.50c.



(b) Projections of 0.035-inch diameter at 0.65c.

Figure 9.- Boundary-layer transition parameter as a function of Reynolds number for low-drag airfoil 1 with projections of various sizes and chordwise locations.

NATIONAL ADVISORY
COMMITTEE FOR AERONAUTICS

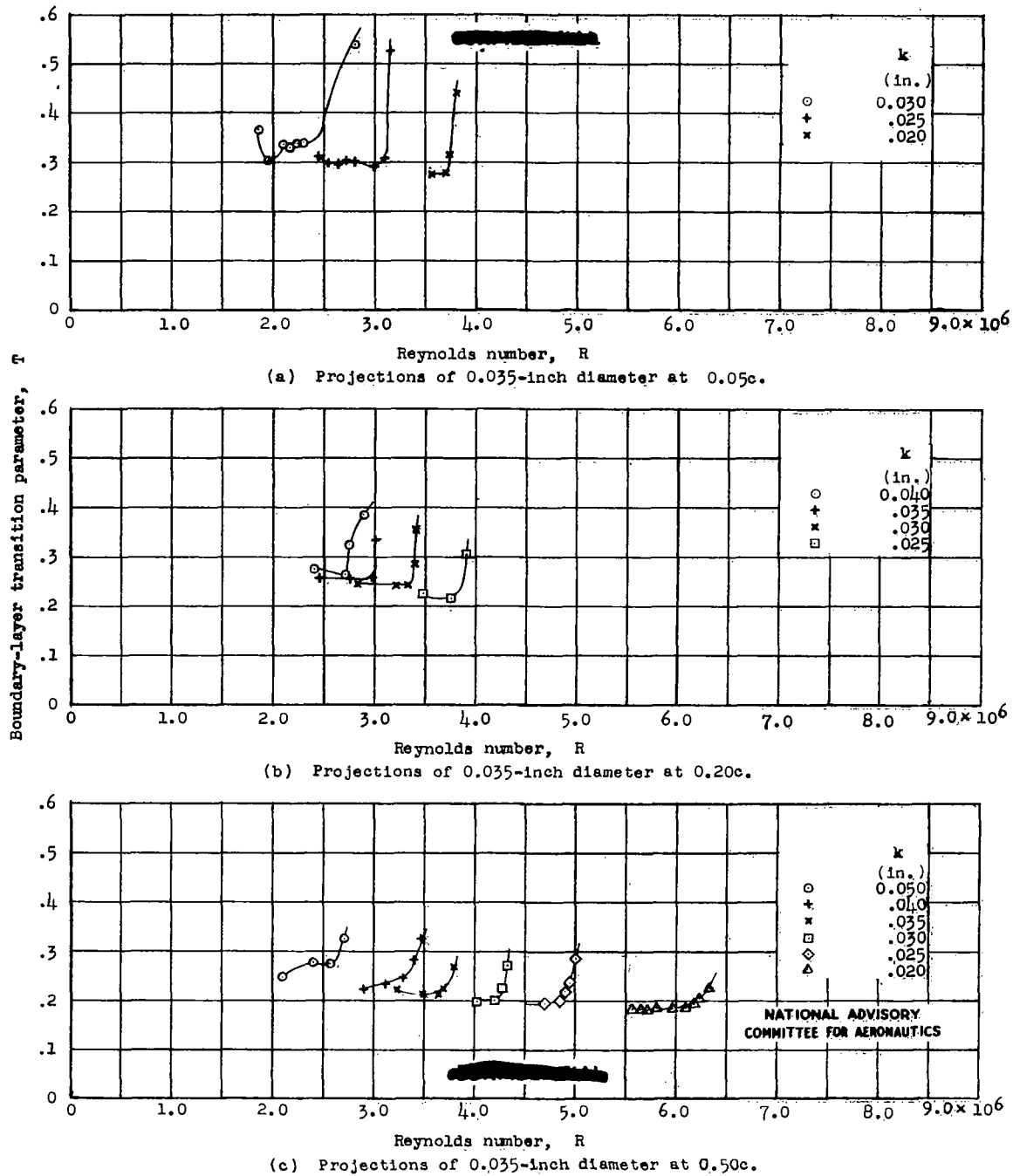


Figure 10.- Boundary-layer transition parameter as a function of Reynolds number for low-drag airfoil 2 with projections of various sizes and chordwise locations.

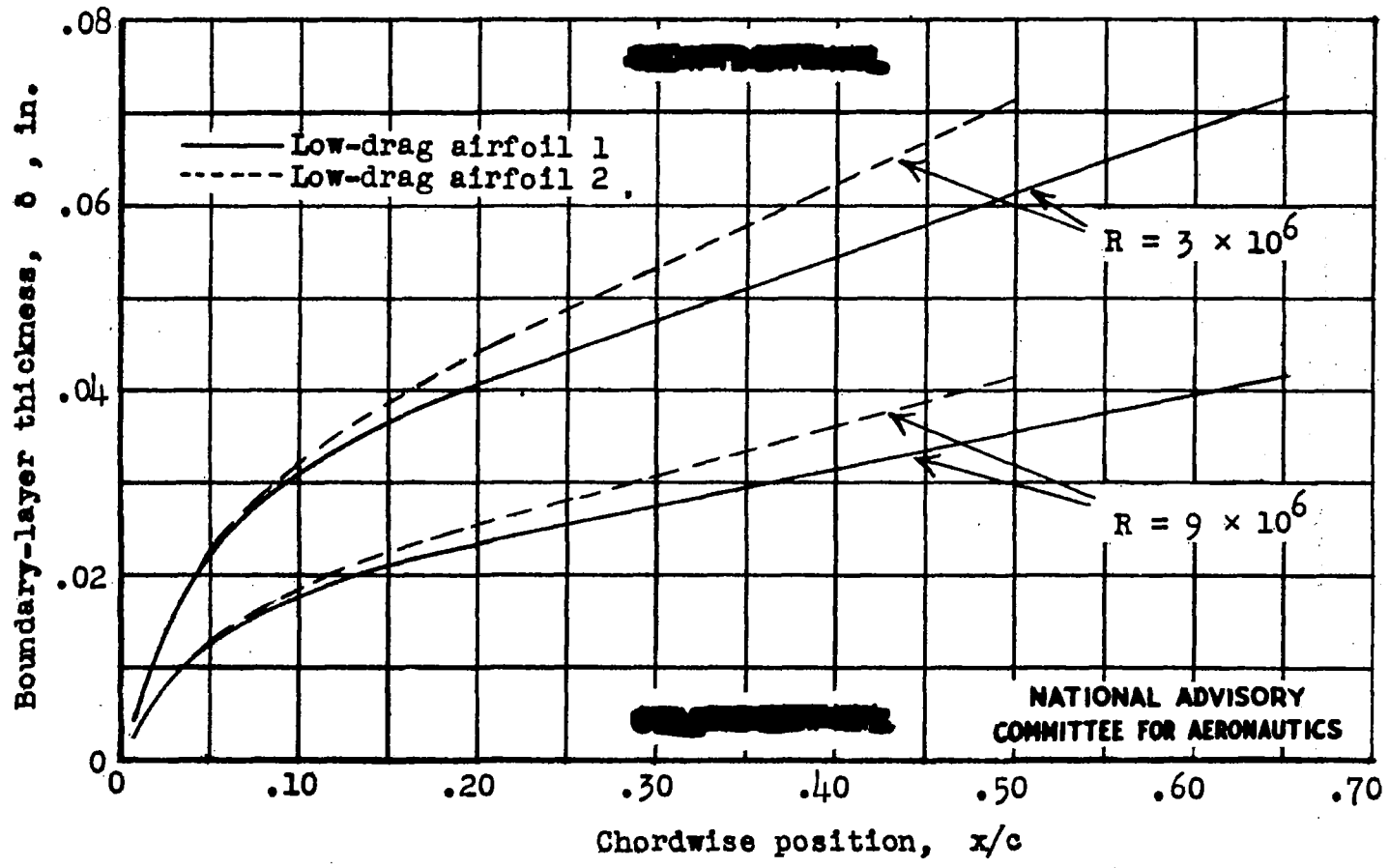
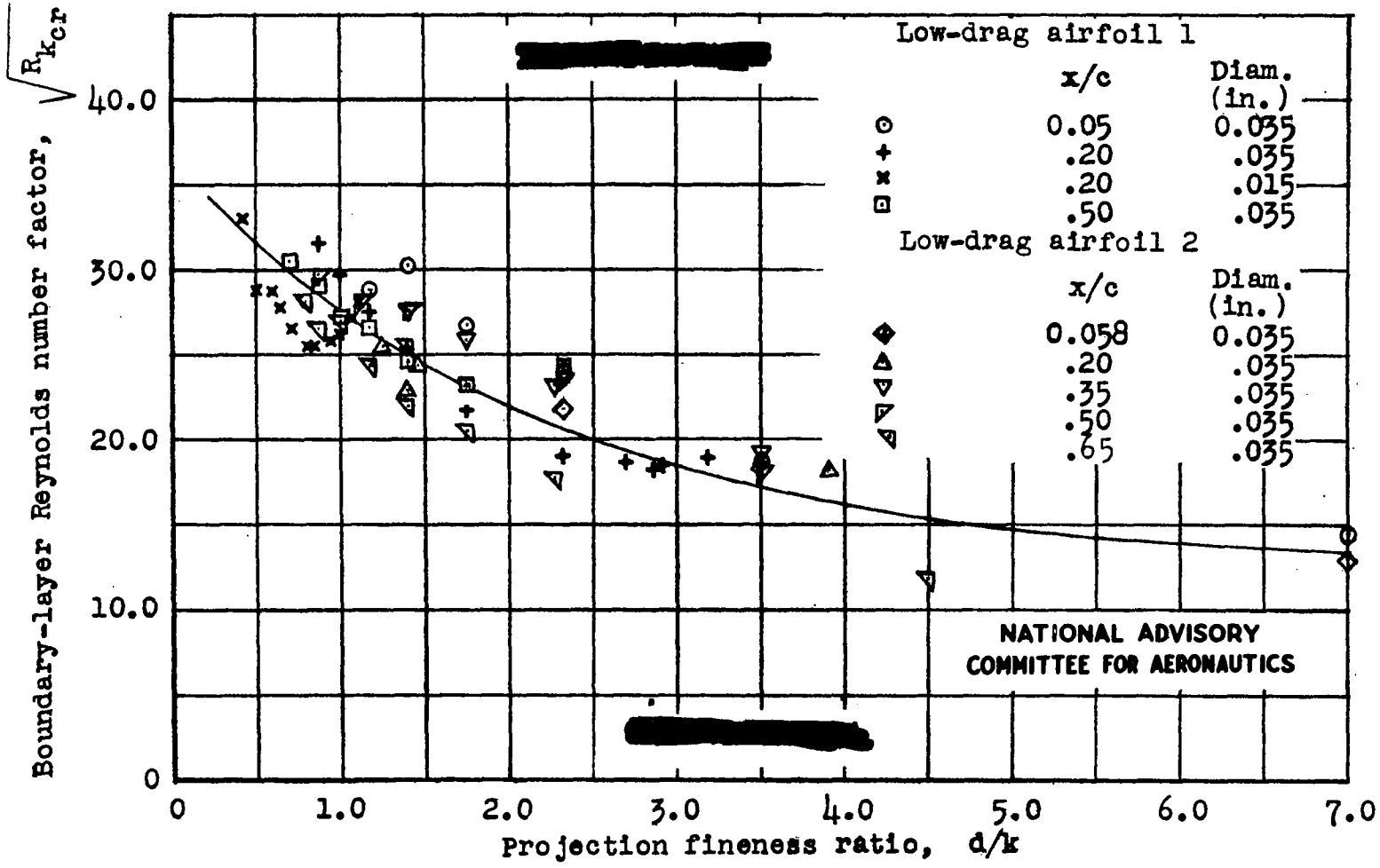


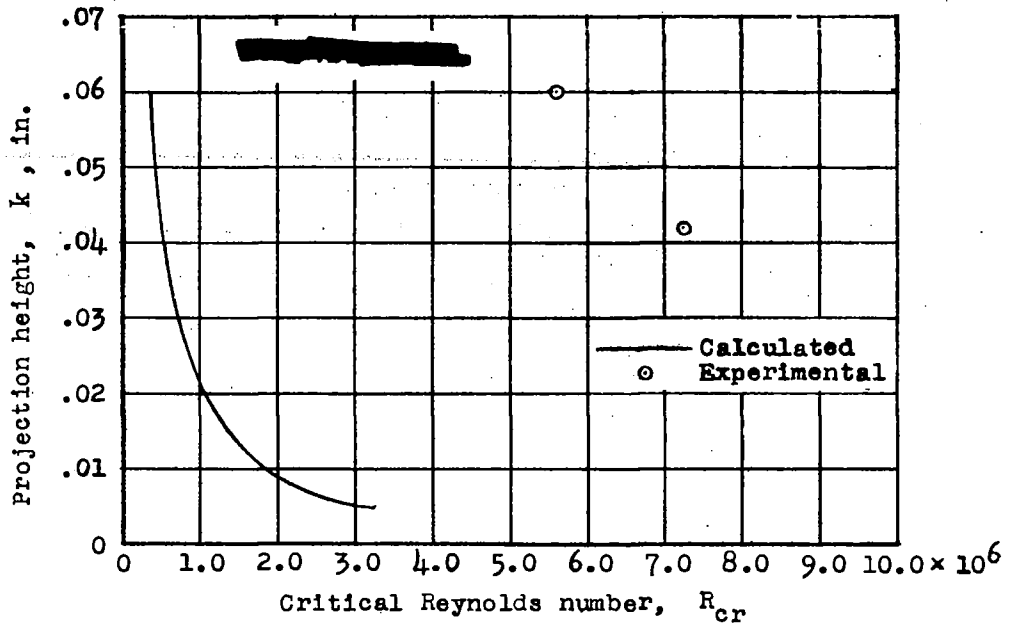
Figure 11.- Variation with chordwise position of upper-surface boundary-layer thickness (calculated by means of equation (B1) of appendix B) on low-drag airfoils 1 and 2 for Reynolds numbers of 3×10^6 and 9×10^6 .

NATIONAL ADVISORY
COMMITTEE FOR AERONAUTICS

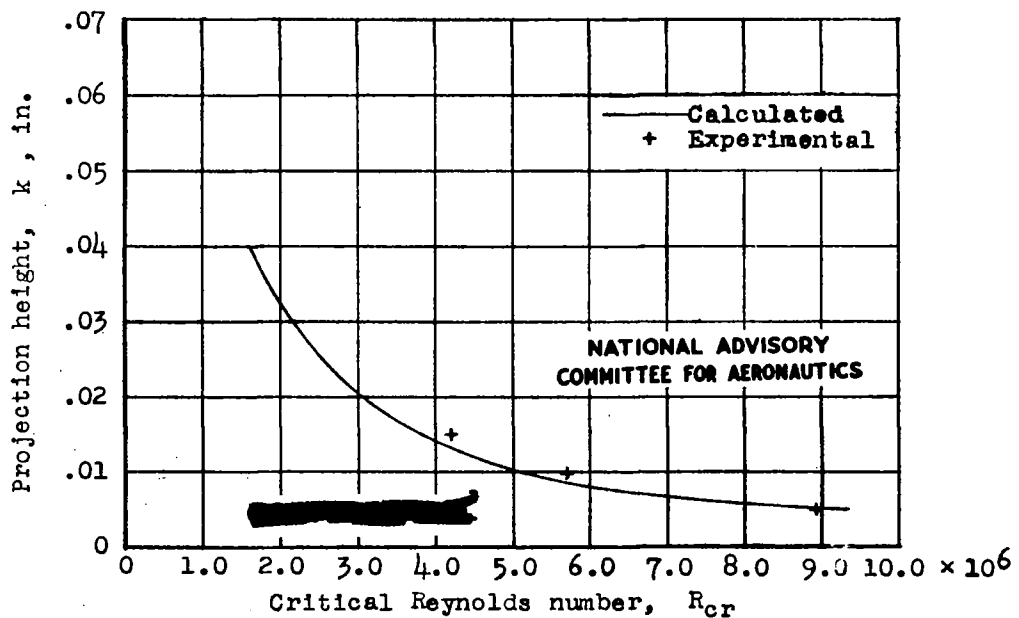


NATIONAL ADVISORY
COMMITTEE FOR AERONAUTICS

Figure 12 .- Variation of boundary-layer Reynolds number factor with projection fineness ratio for low-drag airfoils 1 and 2.

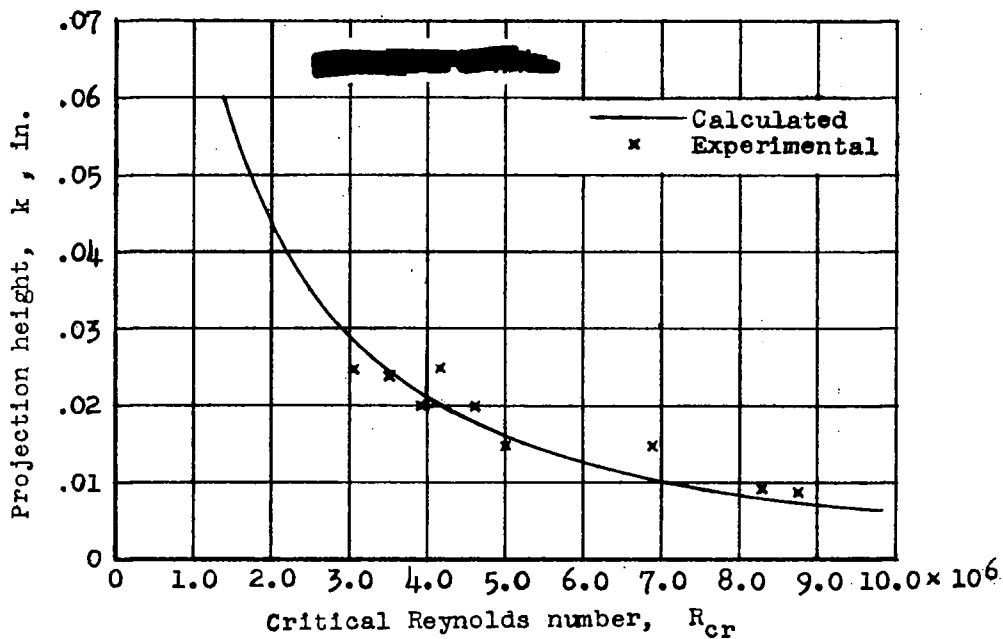


(a) Projections at 0.0007c.

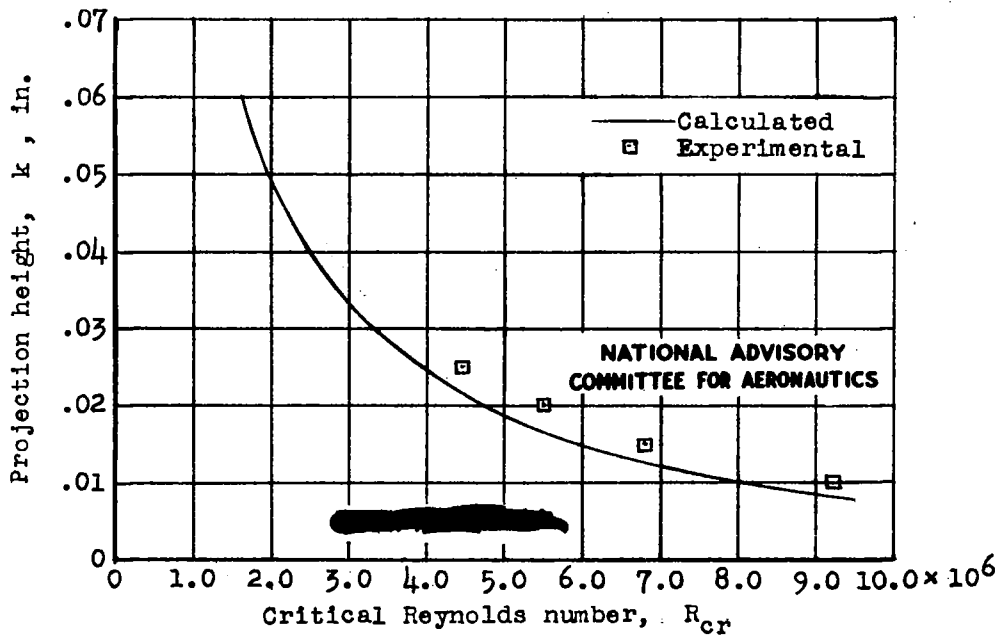


(b) Projections at 0.058c.

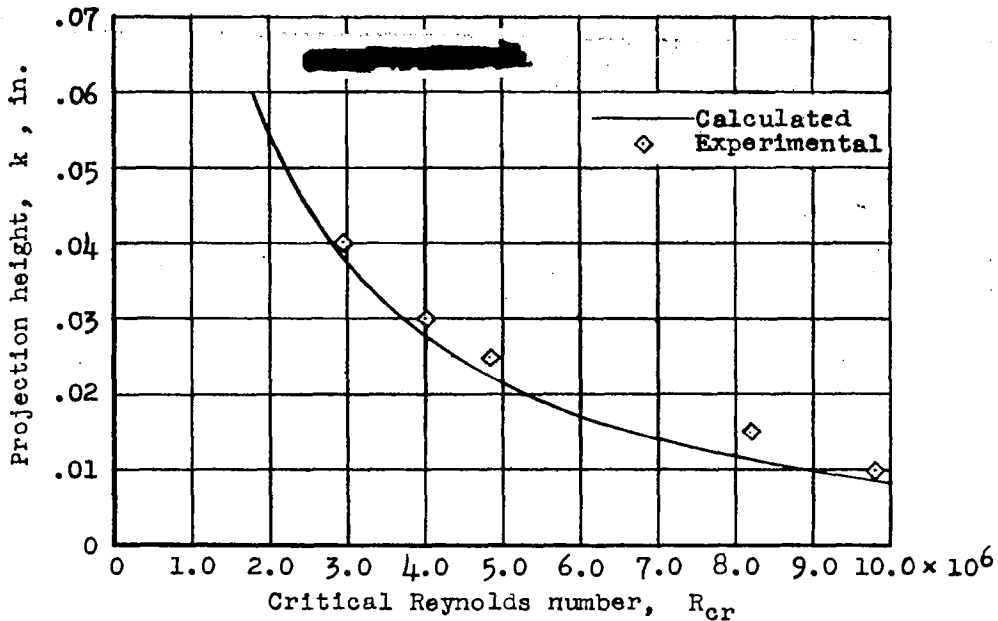
Figure 13 .- Calculated and experimental values of maximum allowable projection height as a function of Reynolds number for projections of 0.035-inch diameter at various chordwise locations on a 90-inch-chord model of low-drag airfoil 1.



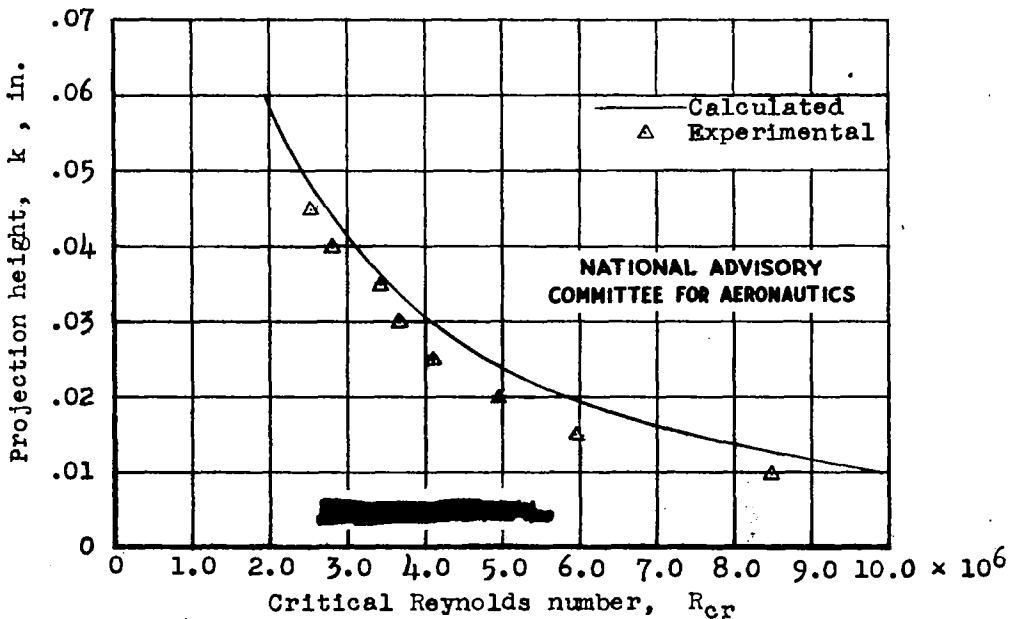
(c) Projections at 0.20c.



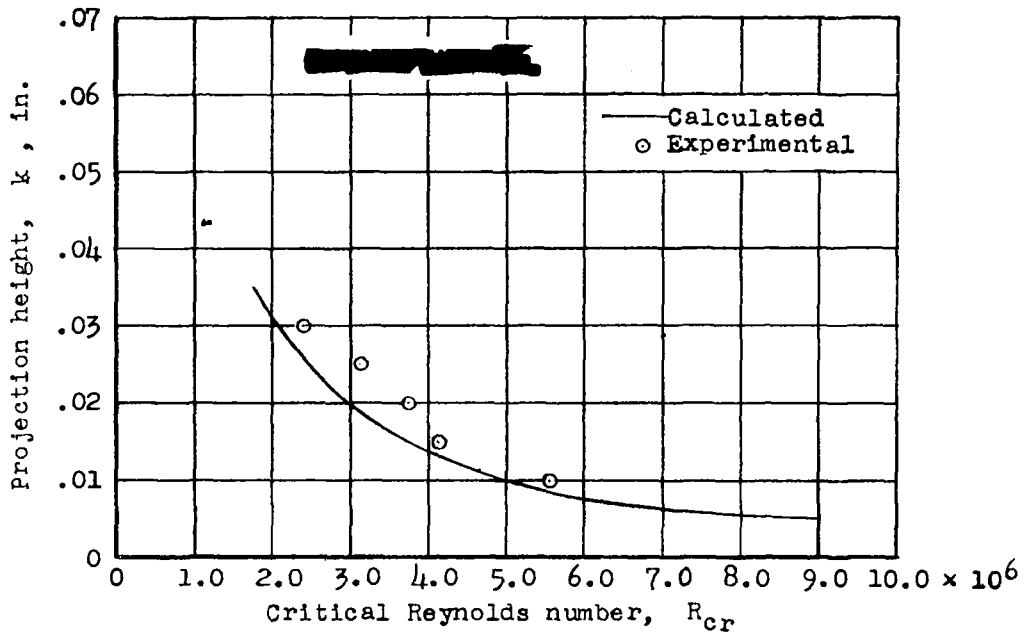
(d) Projections at 0.35c.



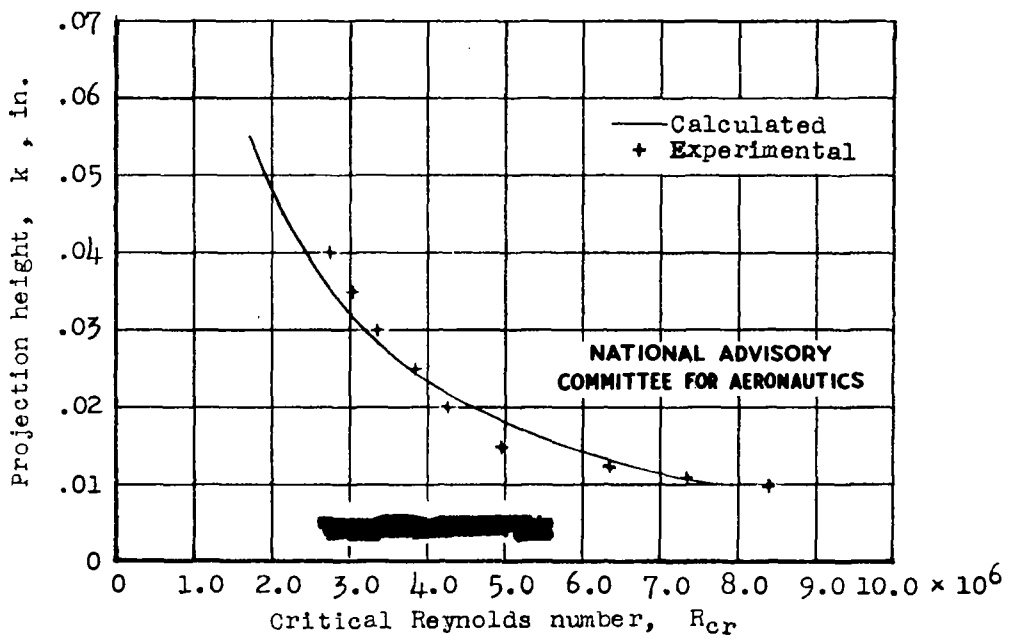
(e) Projections at 0.50c.



(f) Projections at 0.65c.

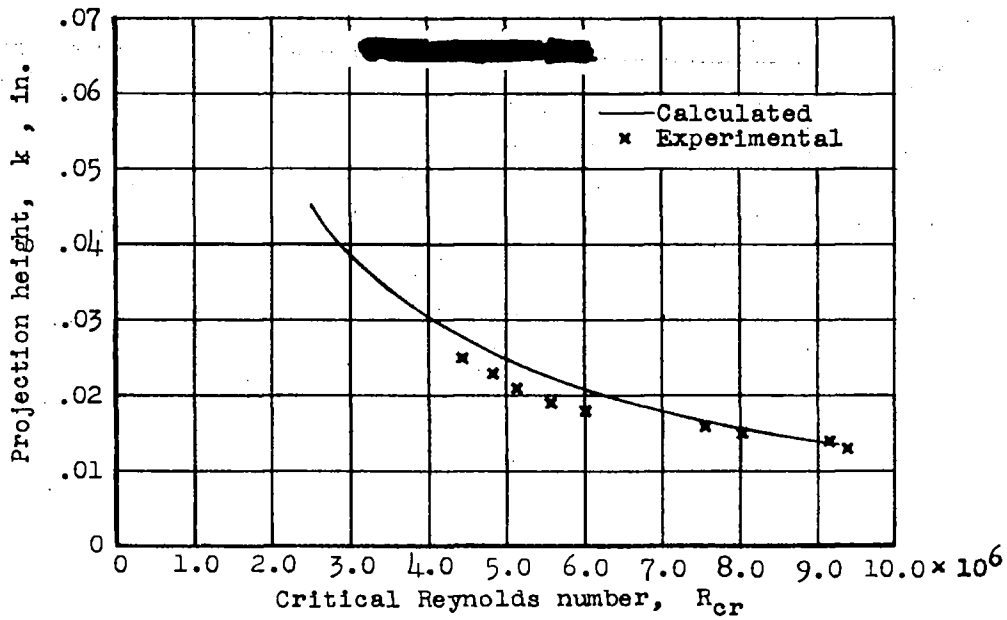


(a) Projections 0.035 inch in diameter at 0.05c.

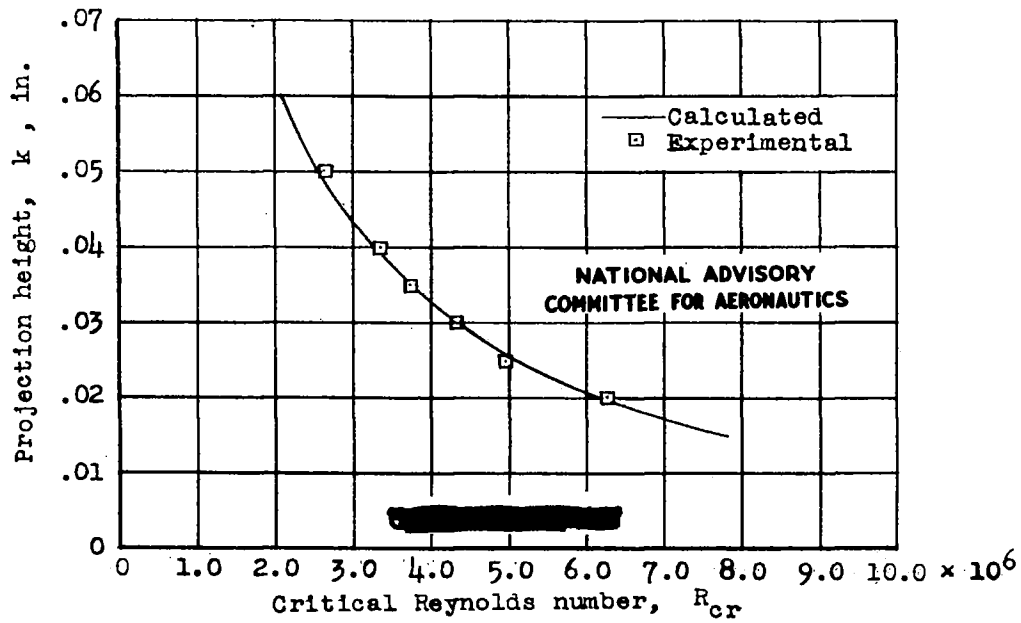


(b) Projections 0.035 inch in diameter at 0.20c.

Figure 14 .- Calculated and experimental values of maximum allowable projection height as a function of Reynolds number for projections at various chordwise locations on a 90-inch-chord model of low-drag airfoil 2.



(c) Projections 0.015 inch in diameter at 0.20c.



(d) Projections 0.035 inch in diameter at 0.50c.

Figure 14 .- Concluded.

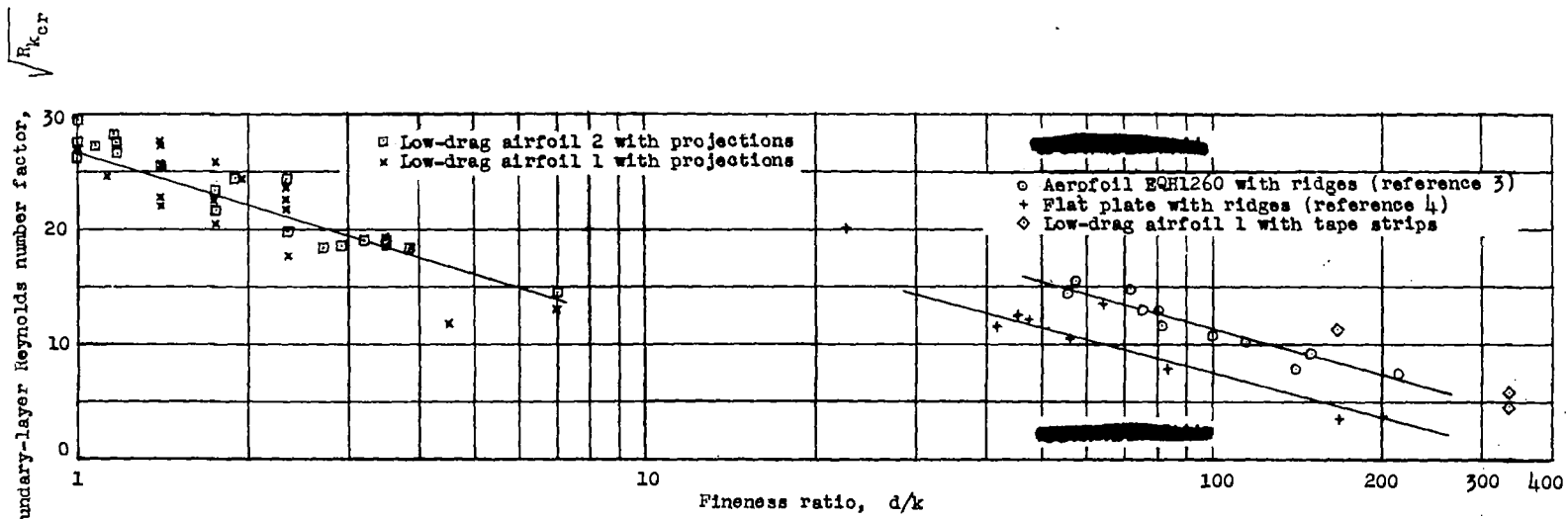


Figure 15.- Variation of boundary-layer Reynolds number factor with fineness ratio for three low-drag airfoils and a flat plate. (The symbol d refers to both ridge width and projection diam.)

NATIONAL ADVISORY
COMMITTEE FOR AERONAUTICS

TITLE: Effects of Specific Types of Surface Roughness on Boundary-Layer Transition

AUTHOR(S): Loftin, L. K.

ORIGINATING AGENCY: National Advisory Committee for Aeronautics, Washington, D. C.

PUBLISHED BY: (Same)

ATI- 8167

REVISION

(None)

ORIG. AGENCY NO.

ACR-15129a

PUBLISHING AGENCY NO.

DATE	DOC. CLASS.	COUNTRY	LANGUAGE	PAGES	ILLUSTRATIONS
Feb '48	Unclass.	U.S.	Eng.	43	tables, graphs

ABSTRACT:

The Reynolds Number at which surface projections of a given type but of various sizes and chordwise locations, would cause premature transition was determined. This number is primarily a function of the projection geometry and the Reynolds Number based on the height of the projection, and the velocity at the top of the projection. The laminar boundary is more sensitive to surface projections than to surface grooves or sanding scratches.

DISTRIBUTION: Request copies of this report only from Originating Agency

DIVISION: Aerodynamics (2)

SECTION: Boundary Layer (5)

SUBJECT HEADINGS: Boundary Layer - Surface Roughness
Effect (18335)

ATI SHEET NO.: R-2-5-t8

Air Documents Division, Intelligence Department
Air Materiel Command

AIR TECHNICAL INDEX

Wright-Patterson Air Force Base
Dayton, Ohio